Inorganic Chemistry

pubs.acs.org/IC

Article

Synthesis, Structure, and Photophysical Properties of Platinum(II) (*N*,*C*,*N*′) Pincer Complexes Derived from Purine Nucleobases†

Carmen Lorenzo-Aparicio, Sonia Moreno-Blázquez, Montserrat Oliván, Miguel A. Esteruelas, Mar Gómez Gallego,* Pablo García-Álvarez, Javier A. Cabeza, and Miguel A. Sierra*

Cite This: *Inorg. Chem.* 2023, 62, 8232–8248

Read Online

ACCESS | Metrics & More | Article Recommendations | Supporting Information

ABSTRACT: The synthesis of a series of Pt{κ^3-*N*,*C*,*N*′-[L]}X (X = Cl, RC≡C) pincer complexes derived from purine and purine nucleosides is reported. In these complexes, the 6-phenylpurine skeleton provides the *N*,*C*-cyclometalated fragment, whereas an amine, imine, or pyridine substituent of the phenyl ring supplies the additional *N*′-coordination point to the pincer complex. The purine *N*,*C*-fragment has two coordination positions with the metal (*N*1 and *N*7), but the formation of the platinum complexes is totally regioselective. Coordination through the *N*7 position leads to the thermodynamically favored [6.5]-Pt{κ^3-*N*7,*C*,*N*′-[L]}X complexes. However, the coordination through the *N*1 position is preferred by the amino derivatives, leading to the isomeric kinetic [5.5]-Pt{κ^3-*N*1,*C*,*N*′-[L]}X complexes. Extension of the reported methodology to complexes having both pincer and acetylide ligands derived from nucleosides allows the preparation of novel heteroleptic bis-nucleoside compounds that could be regarded as organometallic models of Pt-induced interstrand cross-link. Complexes having amine or pyridine arms are green phosphorescence emitters upon photoexcitation at low concentrations in CH_2Cl_2 solution and in poly(methyl methacrylate) (PMMA) films. They undergo self-quenching at high concentrations due to molecular aggregation. The presence of intermolecular $\pi-\pi$ stacking and weak Pt···Pt interactions was also observed in the solid state by X-ray diffraction analysis.

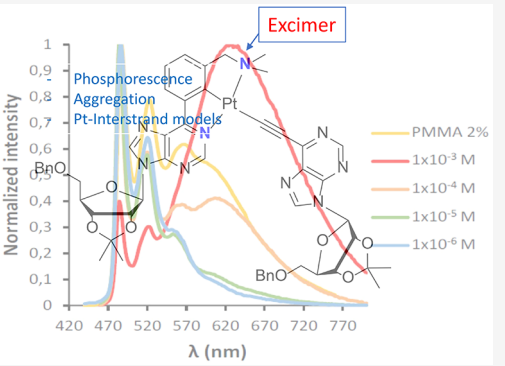

INTRODUCTION

The coordination of DNA fragments to metals is of fundamental importance in many bioinorganic processes.[1] Most of the reported studies in this field focused on the interaction of platinum complexes with DNA and nucleobases, very likely because most of the current antitumor drugs for clinical use are based on platinum complexes.[2−5] The high toxicity of these compounds due to concomitant DNA damage[6] keeps alive the interest for studies that combine Pt and nucleobases to the development of new models of interaction. In this regard, platinum complexes bearing tridentate ligands have attracted particular interest, as they can bind to and intercalate DNA,[7] trigger the formation of G-quadruplexes,[8,9] cause interstrand cross-links (ICL), and generate extensive conformational alterations.[10] The luminescent properties associated with many of these complexes[11−14] have helped the study of interaction models[15,16] and have also been used to investigate intracellular processes *in vivo*.[17]

Our research group is a pioneer in the development of methodologies to prepare cyclometalated transition metal complexes [M = Ir(III), Rh(III), Os(IV)] derived from nucleobases, nucleosides, and nucleotides.[18−21] In these studies, purine derivatives were excellent substrates to carry out cyclometalation reactions, and we reasoned that they could be interesting scaffolds to build cyclometalated platinum(II) (pincer) complexes. The idea was challenging, as purine nucleobase derivatives are highly functionalized systems with many positions prone to interact with the metal.

Most of the reported tridentate cyclometalated platinum(II) complexes are derived from symmetrical ligands. This is remarkable, as unsymmetrical *N*,*C*,*N*′-pincer ligands would offer a great opportunity to tune the properties of the platinum complex by combining the steric and electronic characteristics of the donor N and N′ atoms. In our approach, the 6-phenylpurine skeleton would provide the rigid framework to build unsymmetrical *N*,*CH*,*N*′-pro-ligands **I** (Figure 1) by incorporation of the adequate N′-branches in the phenyl ring. Pro-ligands **I** offer two possible coordination modes to the metal since both *N*1 and *N*7 can bind to form isomers **II** and **III**, respectively. Our previous results showed that cyclometalation reactions of 6-phenylpurine derivatives promoted

Received: February 27, 2023
Published: May 18, 2023

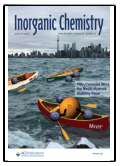

https://doi.org/10.1021/acs.inorgchem.3c00650
Inorg. Chem. 2023, 62, 8232−8248

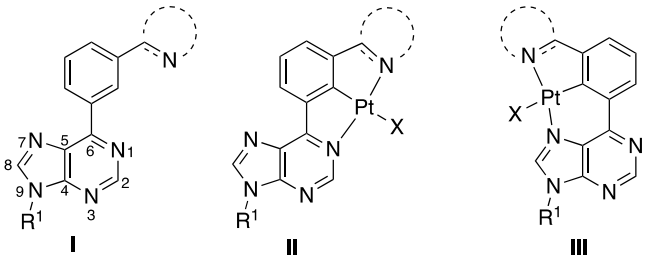

Figure 1. 6-Phenylpurine pro-ligands (**I**) and the isomeric unsymmetrical *N,C,N′*-Pt(II) complexes (**II** and **III**).

by group 8 and group 9 metal complexes exclusively involve the *N*1 atom of the nucleobase in the process of metallacycle formation.[19−21] However, the coordination of *N*7 to many Pt(II) complexes is well known,[2−5] whereas the participation of *N*7 in C-metalations has also been reported.[22]

The donor monodentate ligand (X) that occupies the fourth coordination position of isomers **II** and **III** will also be relevant for the chemical and photophysical properties of the complexes now reported. The trans effect of the cyclometalated carbon is behind the lability of the Pt−Cl bond in Pt{κ^3-*N,C,N′*-[L]}Cl complexes, which will allow us to make further structural modifications by incorporation of diverse alkynyl ligands. Here, we describe the synthesis, reactivity, and the study of the photophysical properties of a new class of Pt{κ^3-*N,C,N′*-[L]}X (X = Cl, RC≡C) complexes, derived from biomolecules: purine nucleobases and nucleosides. The methodology reported in this work is a step ahead in the design of a new class of photoluminescent complexes built on biocompatible moieties. Combination, in the metal coordination sphere, of a pincer containing a purine nucleoside arm together with purine nucleoside-substituted alkynyl ligands will allow us to furthermore generate complexes that can be viewed as organometallic interstrand cross-link models. In this context, it should be mentioned that interstrand cross-link is one of the most important pathways for DNA damage.[10]

RESULTS AND DISCUSSION

Scheme 1 summarizes the preparation of the *N,CH,N′*-pro-ligands **2a−c**. The synthesis of **2a** and **2b** was designed in a stepwise manner using a common precursor, aldehyde **1**. This compound was generated through a Suzuki coupling between 6-chloro-9-ethylpurine and 3-formylboronic acid, using Pd(PPh$_3$)$_4$ as a catalyst precursor and K_2CO_3 as a co-catalytic base. Amine **2a** was generated by reductive amination of **1**, with dimethylamine and $NaBH_3CN$, using Ti(O^{i}Pr)$_4$ as a catalyst; while imine **2b** was made by the reaction of **1** with *p*-anisidine. In turn, pyridine derivative **2c** was synthesized in one step from 6-chloro-9-ethylpurine by Pd(PPh$_3$)$_4$/K_2CO_3-mediated Suzuki coupling with 3-(2-pyridynyl)phenylboronic acid pinacol ester.

Pro-ligands **2a−c** were subsequently used to prepare the respective chlorido-complexes Pt{κ^3-*N,C,N′*-[L]}Cl: **3a−c**. The synthetic procedure involves the reaction of the salt K_2PtCl_4 with the organic molecules, in glacial acetic acid, under reflux (Scheme 2).[23] Complexes **3a** and **3b** were obtained as pure products in 56 and 46% isolated yields, respectively, after chromatography of the reaction crude on silica gel. In contrast, complex **3c** was directly obtained (52% yield) by precipitation from the reaction medium with methanol and subsequent washing with methanol and diethyl ether. The three compounds were characterized by NMR spectroscopy and X-ray diffraction (XRD) analysis. The main bond distances and angles are given in Table S1.

Figure 2 shows views of the molecules. The ligand environment around the platinum(II) center adopts the expected square-planar coordination, featuring a tridentate κ^3-*N,C,N′*-ligand and a chloride anion trans to the metalated carbon atom. The atoms of the 6-phenylpurine scaffold are roughly coplanar in all cases. It should be pointed out that the

Scheme 1. Synthesis of Pro-ligands 2a−c

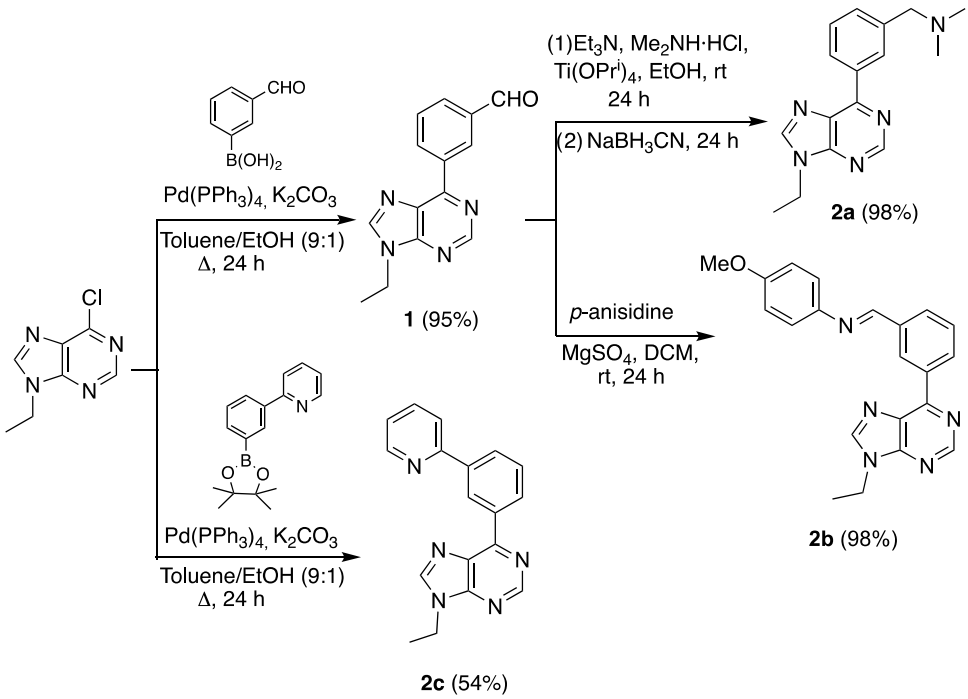

https://doi.org/10.1021/acs.inorgchem.3c00650
Inorg. Chem. 2023, 62, 8232−8248

Scheme 2. Synthesis of Complexes 3a–c

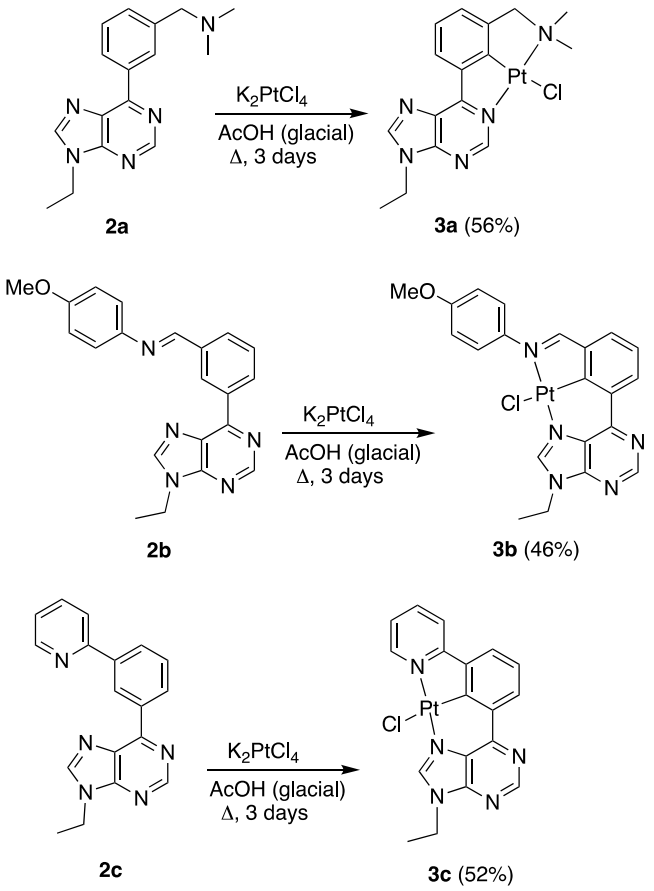

purine arm coordinates the platinum atom by the *N*1 position in **3a**, while the coordination occurs through the *N*7 atom in **3b** and **3c**. In the first case, a five-membered heterometallacycle is generated, resulting in a [5.5]-Pt{κ^3-*N*,*C*,*N*′-[L]}Cl bicycle derivative. By contrary, the *N*7 coordination gives rise to a six-membered heterometallacycle, which affords a [6.5]-Pt{κ^3-*N*,*C*,*N*′-[L]}Cl bicycle. The N–Pt–N′ angles of complexes **3b** and **3c** are closer to the ideal value of 180° (average 173(1)°) than in **3a** (162.2(2)°) due to the strain imposed by the five-membered ring in the latter. All complexes show C9–Pt–Cl angles very close to 180° (average 176.8(5)°) and similar Pt–N, Pt–C, and Pt–Cl bond distances, which are in the range of those reported for related Pt{κ^3-*N*,*C*,*N*-[L]}Cl complexes.[24]

Inspection of the packing within the crystals of complexes **3a** (Figure 3), **3b** (Figure S1), and **3c** (Figures 4 and S2) reveals that the planes defined by the 6-phenylpurine scaffolds are close to each other (less than 4 Å) and arranged in an approximately or totally parallel manner, which points to the existence of intermolecular $\pi-\pi$ stacking interactions. The asymmetric units contain four (two pairs in **3a**) or two close molecules (**3c**), which in the crystal generate stacks, with Pt···Pt distances of 3.835–3.861 Å for **3a** and 4.279 Å for **3c**; indicating the existence of significant metal–metal interactions (Figure 3).[25] The asymmetric units of complex **3b** contain only one molecule (see the Supporting Information (SI)), and the closest intermolecular Pt···Pt distance in the crystal is 6.750 Å, longer than 2 × r_{vdw}(Pt) = 4.6 Å,[26] which rules out the existence of significant metal–metal interactions in this case.

The study of the ^{1}H NMR spectra was congruent with the crystal structures. The coordination through the *N*7 position of the purine ring in complexes **3b** and **3c** was confirmed by the noticeable deshielding of the signals of purine *H*8, from 8.17 ppm in pro-ligands **2b** and **2c** to 9.29 (J_{H-Pt} = 11.2 Hz) and 9.37 ppm (J_{H-Pt} = 14.2 Hz) for **3b** and **3c**, respectively. However, in complex **3a**, the signal coupled to the neighboring platinum in the ^{1}H NMR spectrum was that of purine *H*2 (9.40 ppm, J_{H-Pt} = 11.5 Hz), being also deshielded with regard to that of pro-ligand **2a** (8.98 ppm).

The *N*1 coordination of the purine arm in **3a** is in line with our previous results in Ir(III)-, Rh(III)-, and Os(IV)-chemistry, which pointed out that only the *N*1 position of the purine ring was involved in the cyclometalation reactions of 6-phenylpurine derivatives, on complexes of these ions.[19,21] To understand the difference in behavior between the pro-ligands, we analyzed the equilibrium between the isomers [5.5]-Pt{κ^3-*N*,*C*,*N*′-[L]}Cl and [6.5]-Pt{κ^3-*N*,*C*,*N*′-[L]}Cl by density functional theory (DFT) calculations (B3LYP-D3/def2-SVP) (Figures S7–S9). The first analysis of the computed data revealed that the isomer [6.5]-Pt{κ^3-*N*,*C*,*N*′-[L]}Cl is more stable than the [5.5]-Pt{κ^3-*N*,*C*,*N*′-[L]}Cl, in all cases. That is, the *N*7 coordination of the purine arm is

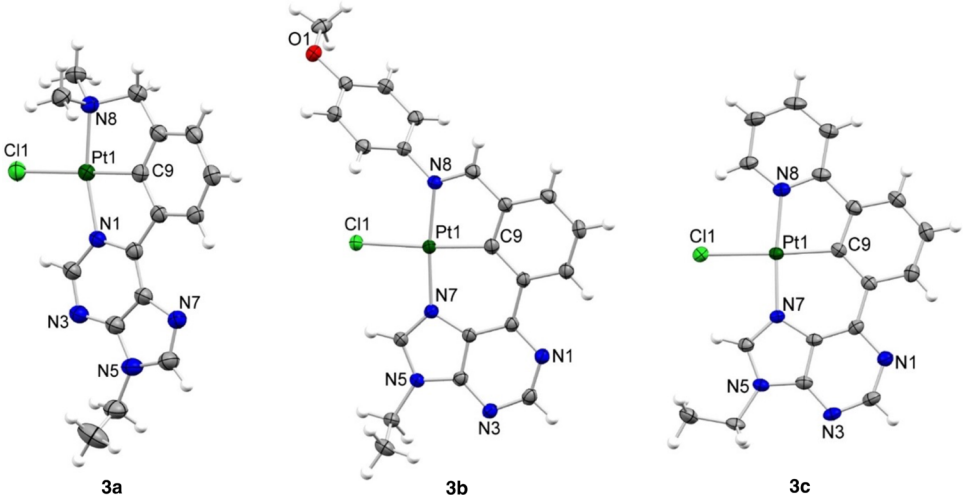

Figure 2. Molecular structures of complexes **3a–c** (30% displacement ellipsoids).

https://doi.org/10.1021/acs.inorgchem.3c00650
Inorg. Chem. 2023, 62, 8232–8248

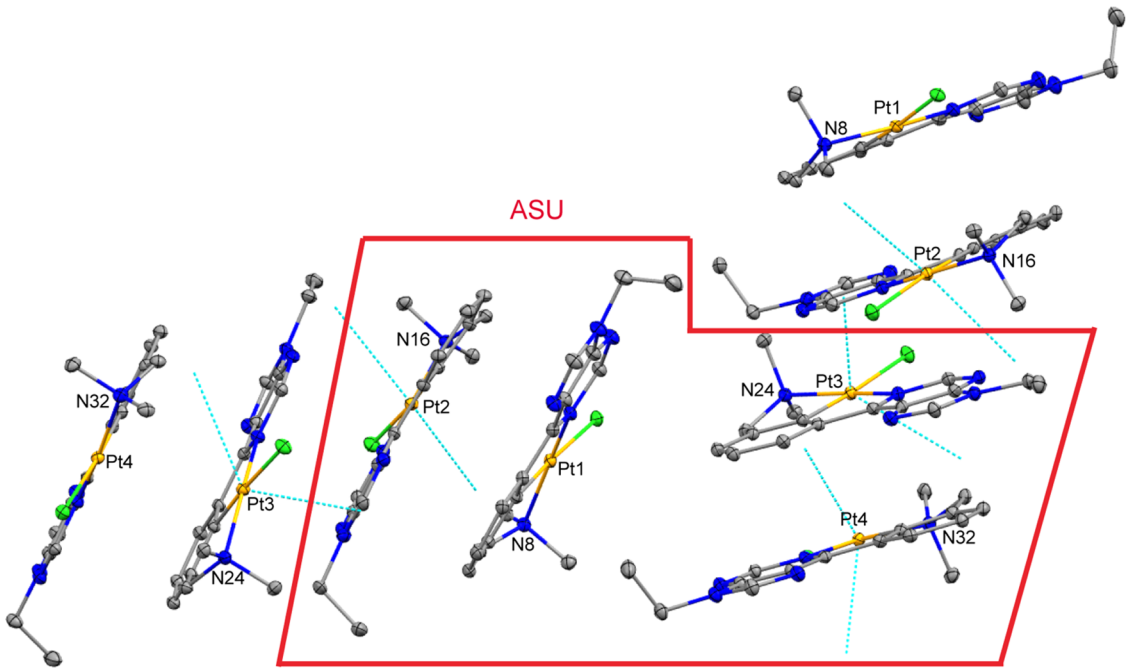

Figure 3. View of two groups of four molecules found in the crystal of **3a** (10% displacement ellipsoids), showing the approximate parallel disposition of the planes defined by the 6-phenylpurine scaffolds (separated by 3.3(3) Å (Pt1···Pt2), 3.4(3) Å (Pt3···Pt4), and 3.6(3) Å (Pt2···Pt3)). The shortest Pt···Pt distances are 3.835 Å (Pt1···Pt2) and 3.861 Å (Pt3···Pt4). The Pt2···Pt3 distance is 9.467 Å. The asymmetric unit (ASU) contains four molecules.

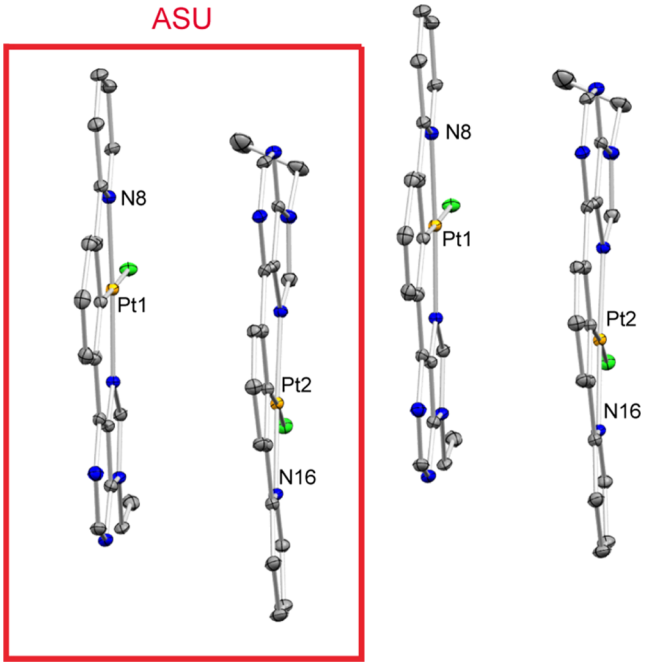

Figure 4. View of the molecular arrangement of **3c** in the crystal (10% displacement ellipsoids), showing the approximate parallel disposition of the planes defined by the 6-phenylpurine scaffolds [separated by 3.48(5) Å (within the asymmetric unit) and 3.38(5) Å (between molecules of different asymmetric units)]. This approximate parallel orientation is maintained along the entire crystal lattice. The shortest Pt···Pt distances are 4.279 Å (between the molecules of the asymmetric unit) and 5.141 Å (between molecules of different asymmetric units). The asymmetric unit (ASU) contains two molecules.

thermodynamically favored over the coordination through *N*1 (between 9.01 and 10.38 kcal mol^{-1}). In consequence, complex **3a** must be regarded as the kinetic product of the reaction of **2a** with the platinum salt. A more detailed DFT analysis showed that the transformation **3a** into the more stable isomer, [6.5]-Pt{κ^3-*N*,*C*,*N*′-[L]}Cl, **3d** takes place in two stages (Figure 5), via the three-coordinate intermediate **I1** (dihedral angle Ca−Cb−Cc−Cd 49.70°). The first stage involves the rupture of the *N*1−Pt bond via the transition state **TS1**, whereas the formation of the *N*7−Pt bond occurs in the second step through the transition state **TS2**. The activation energies of both steps are 29.6 and 31.2 kcal mol^{-1}, respectively, considering acetic acid as the solvent. These barriers increase up to 33.0 and 35.8 kcal mol^{-1} in toluene.

Based on these studies, we first tested the isomerization **3a** to **3d** in acetic acid, at 200 °C, in a sealed tube. Unfortunately, complete decomposition to a black solid occurred. Thence, we tried the process in toluene. To our delight, this time, the clean and quantitative transformation of **3a** into the more stable species **3d** took place after 120 h (Scheme 3). In agreement with **3b** and **3c**, the ^{1}H NMR spectrum of **3d** showed a clean singlet at 8.99 ppm due to H2, while the signal corresponding to H8 showed platinum satellites ($^3J(^1\mathrm{H}-^{195}\mathrm{Pt})$ = 10.5 Hz). The formation of **3d** was confirmed by XRD. Inspection of the crystal packing did not reveal significant Pt···Pt interactions in this case (Scheme 3 and Figure S3).

The chloride ligand of complexes **3a−d** was further replaced by acetylide ligands. Reaction with phenylacetylene, in the presence of NaOH, at room temperature (rt), in methanol led to acetylido derivatives **4a−d**, which were isolated as yellow-orange solids in 65−79% yields by precipitation in the reaction media and subsequent washing with cold methanol and diethyl ether (Scheme 4). Extension of this methodology to more sensitive acetylide ligands was tested by the reaction of **3a−d** with freshly prepared 6-ethynyl-9-ethylpurine. In this case,

https://doi.org/10.1021/acs.inorgchem.3c00650
Inorg. Chem. 2023, 62, 8232−8248

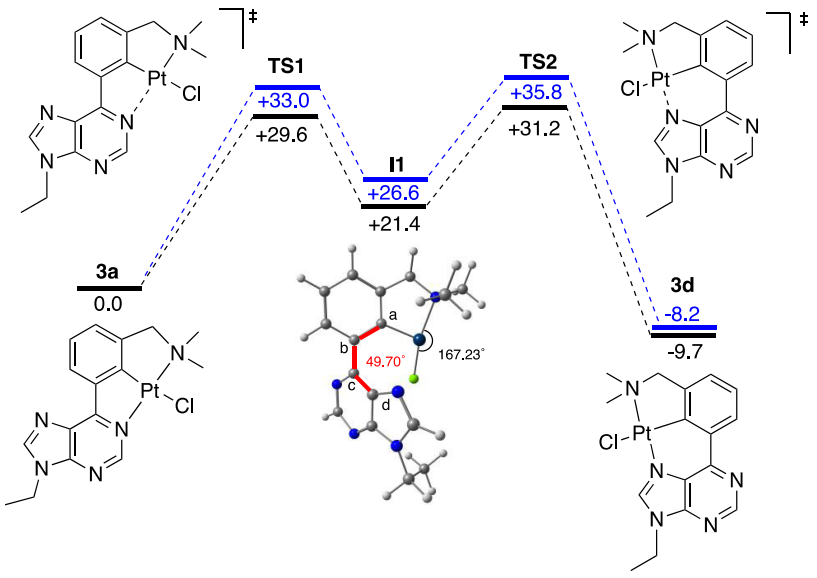

Figure 5. Energy profiles for the isomerization of **3a** to **3d** (B3LYP-D3/def2-SVP) in acetic acid (black) and toluene (blue). Relative energy values at 298 K (kcal mol^{-1}).

Scheme 3. Isomerization of 3a to 3d and Molecular Structure of 3d (30% Displacement Ellipsoids)[a]

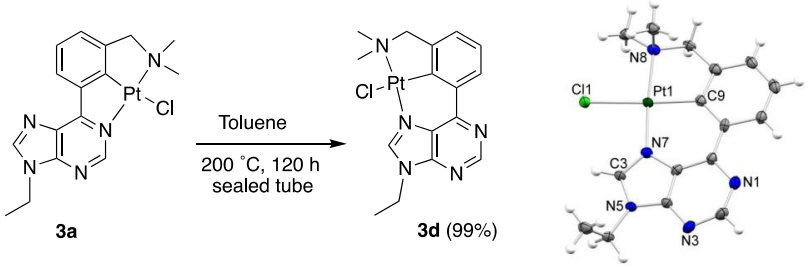

[a]Only one of the two analogous molecules found in the asymmetric unit is shown.

complexes **5a−d** were also obtained in high yields (65−80%) as yellow solids (Scheme 4).

Acetylido derivatives were characterized by NMR and mass spectrometry and, in the case of **4b**, **4d**, and **5a**, by XRD (Scheme 4 and Figures S4−S6). The C≡C bond distances of 1.202(9), 1.190(5), and 1.20(2) Å, respectively, compare well with those reported for the compounds of this class previously characterized by XRD.[27] This fact is indicative of the lack of significant π-back-bonding from the Pt atoms to the alkynyl ligands.

To go a step ahead, we explored this methodology to prepare both types of [5.5]- and [6.5]-Pt{κ^3-*N,C,N′*-[L]}X (X = Cl, RC≡C) pincer complexes in purine nucleosides as ligand precursors (Scheme 5). Pro-ligands **7a** and **7b** were obtained in quantitative yields from aldehyde **6** (see the SI) using the reaction conditions previously employed for the preparation of **3a** and **3b**. However, the synthesis of the respective chlorido compounds [5.5]-Pt{κ^3-*N,C,N′*-[L]}Cl could not be achieved by the reaction of **7a** and **7b** with K_2PtCl_4, in glacial acetic acid, under reflux, as these harsh conditions caused the decomposition of the pro-ligands. Chlorido derivatives **8a** and **8b** were successfully prepared by refluxing **7a** and **7b** with [$PtCl_2$(DMSO)$_2$] (DMSO = dimethyl sulfoxide) in toluene for 48 h, in 49 and 28% yields, after chromatography on silica gel. Further, the reaction of **8a** and **8b** with freshly prepared ethynylpurine nucleoside **9** (see SI) in a NaOH solution in methanol afforded heteroleptic bis-nucleoside compounds **10a** and **10b** in 57 and 41% yields, respectively. Complexes **10a** and **10b** join two purine nucleosides in their structures through the alkynyl−Pt complex and could be regarded as simple organometallic models of interstrand cross-link (ICL) in oligonucleotides.[10]

Photophysical Properties of Emissive Complexes. The square-planar platinum(II) d^8-complexes are considered one of the noble families of phosphorescent emitters.[11−14,28] This fact, along with the novelty of the purine−pincer−platinum(II) skeleton prompted us to study the absorption and emission characteristics of the emissive compounds prepared, which were those of the **3**, **4**, and **5**-types bearing an amine- or pyridine arm (imine derivatives were not emissive).

The UV−vis spectra of complexes **3**, **4**, and **5** (10^{-5} M, in dichloromethane (DCM), at room temperature) are depicted in Figure 6, and the selected absorptions (assigned by time-dependent density functional theory calculations (TD-DFT-B3LYP-D3/def2-SVP) in dichloromethane) are shown in Tables S3−S6. The frontier molecular orbitals of complexes **3−5** are provided in Figures S10−S14. The lowest unoccupied molecular orbitals (LUMOs) are very similar, mainly localized on the cyclometalating (*N,C*) fragments of the pincer ligand. For the chloride complexes **3a−d**, the highest occupied molecular orbitals (HOMOs) are composed of the Pt and halide centers with some contribution of the phenyl moiety. In

https://doi.org/10.1021/acs.inorgchem.3c00650
Inorg. Chem. 2023, 62, 8232−8248

Scheme 4. Synthesis of the Alkynyl Derivatives 4a−d and 5a−d and Molecular Structures of 5a, 4b, and 4d (30% Displacement Ellipsoids)

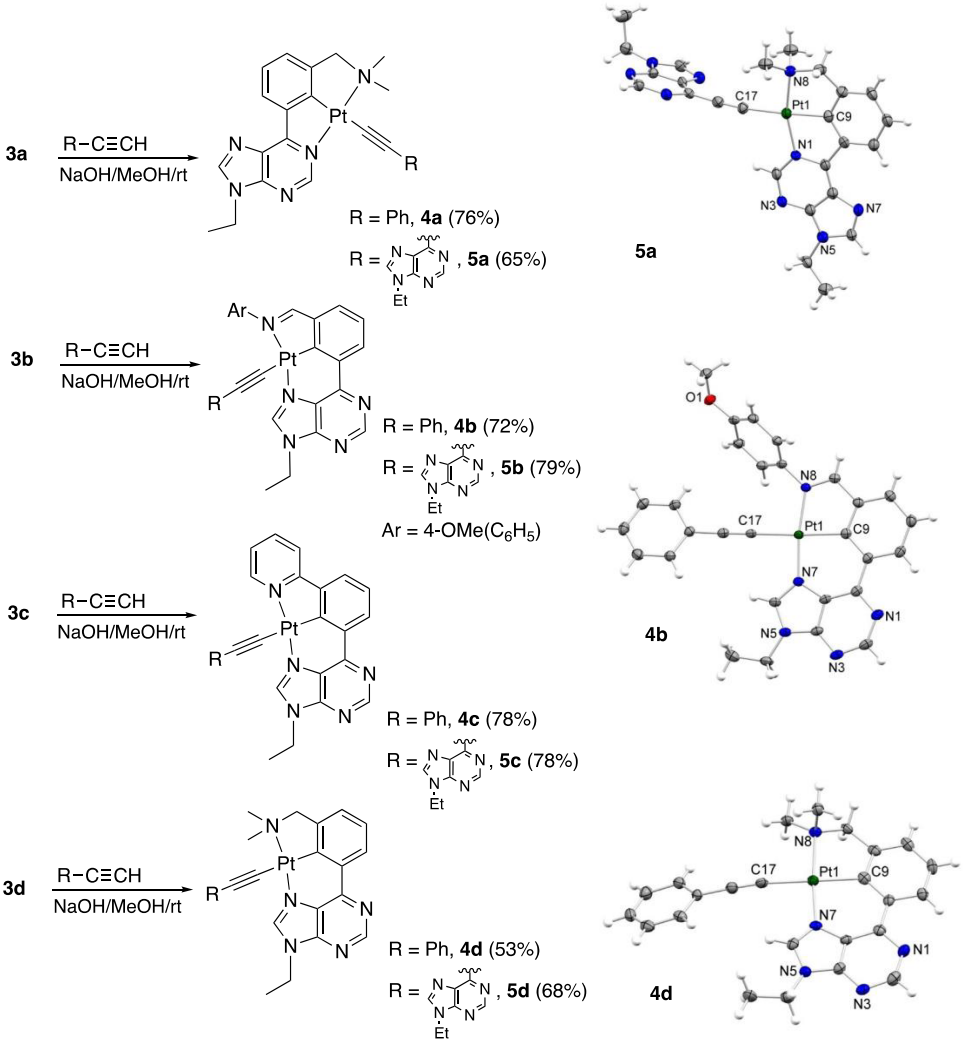

turn, the HOMOs of the acetylide derivatives **4a−d** and **5a−d** are mainly formed by the contribution of the aryl acetylide ligand and the Pt centers. All compounds display intense bands in the region 270−330 nm, with extinction coefficients (ε) of about 10^4 dm^3 mol^{-1} cm^{-1}, which can be assigned to the intraligand IL [$\pi-\pi^*$] transition of the pincer ligand, mixed with metal to ligand charge transfer (MLCT) [dπ(Pt) to $\pi^*(N,C,N')$] transitions. In addition, moderately intense absorption bands were observed at about 390−450 nm with extinction coefficients on the order of 10^3-10^4 dm^3 mol^{-1} cm^{-1}. In the case of the halide derivatives **3a−d**, these absorptions are ascribed to IL [$\pi-\pi^*$] mixed with MLCT [dπ(Pt) to $\pi^*(N,C,N')$] transitions. For acetylide complexes **4a−d** and **5a−d**, those lower energy absorptions are ascribed to LLCT [π(phenylacetylide) to $\pi^*(N,C,N')$] or [π(9-ethylpurineacetylide) to $\pi^*(N,C,N')$] transitions. The very weak bands at lower energy, about 470−550 nm, are attributed to the direct population of the triplet $\pi-\pi^*$ state facilitated by the high spin−orbit coupling associated with the Pt(II) ion. There is a good agreement between the computed selected transitions and the experimental absorption maxima.

Emissions take place upon photoexcitation and occur in the green region of the spectrum (476−571 nm). Measurements were performed in doped poly(methyl methacrylate) films at 5 and 2 wt % ($PMMA_{5\%}$ and $PMMA_{2\%}$) at 298 K and in dichloromethane (CH_2Cl_2) and 2-methyltetrahydrofuran (2-MeTHF) at 298 and at 77 K. Table 1 summarizes the main features of the emissions, which occur from the respective T_1 excited states as supported by the excellent agreement observed between the maximum of the emission wavelengths in CH_2Cl_2 and the calculated values in the same solvent for the differences in energy between the optimized triplet states T_1 and the singlet states S_0. According to the spin density distribution calculated for the T_1 states in their minimum energy geometries (Table S8 and Figures S102−S110), the emissions appear to have a mixed MLTC/LC/LLCT character in all cases. Consistently, the bands are highly structured.

Amine kinetic isomers **3a**, **4a**, and **5a** display moderated quantum yields in $PMMA_{5\%}$ (0.36−0.50). The values significantly increase for the thermodynamic counterparts, which lie in the range 0.70−0.48 and decrease in the sequence **3d** > **4d** > **5d**. Two factors play in favor of the thermodynamic isomers. A comparison of the molecular packing for **3a** and **3d** reveals that the aggregation is higher in the kinetic isomers and is known to favor self-quenching.[29] In addition, increasing emission efficiency with emitter stability is a common effect,

https://doi.org/10.1021/acs.inorgchem.3c00650
Inorg. Chem. 2023, 62, 8232−8248

Scheme 5. Synthesis of Acetylido Complexes 10a and 10b

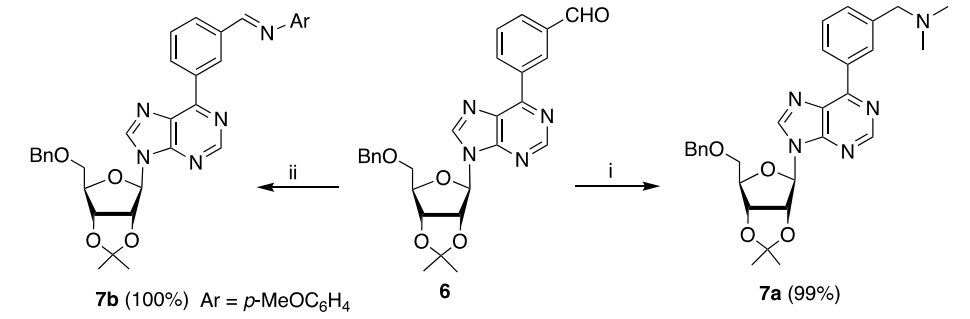

(i) (a)Ti(O^{i}Pr)$_4$, EtOH, Et$_3$N; Me$_2$NH·HCl, 24 h rt; (b) NaBH$_3$CN, 24 h rt; (ii) p-MeOC$_6$H$_4$NH$_2$, DCM, rt, 24 h

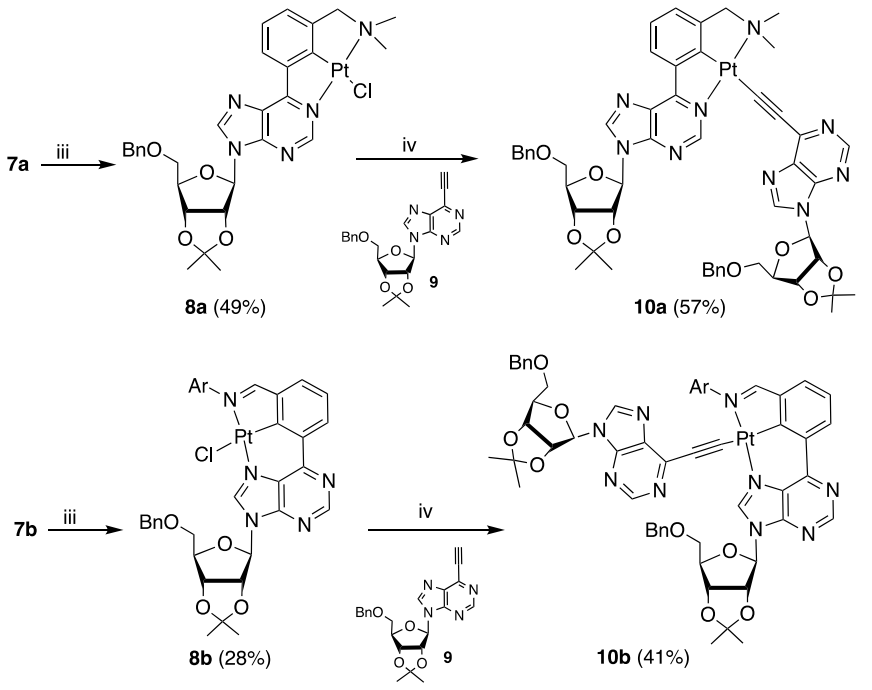

(iii) cis-[PtCl$_2$(dmso)$_2$],toluene, reflux, 5 days; (iv) NaOH, MeOH, rt, 24 h

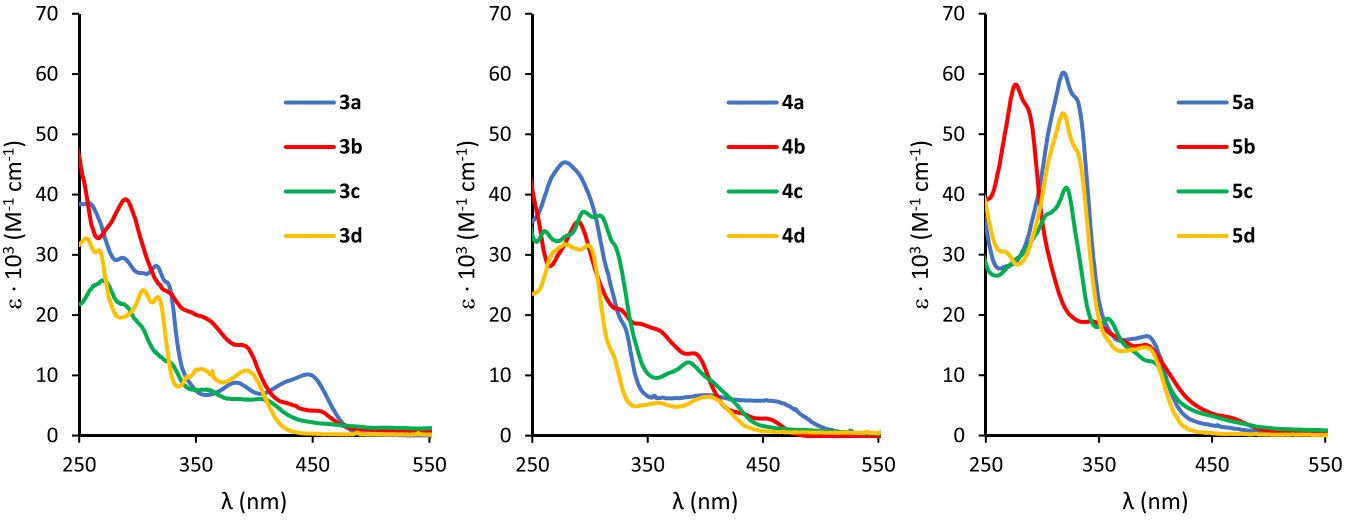

Figure 6. UV−vis spectra of complexes **3a−d** (left), **4a−d** (center), and **5a−d** (right) in CH_2Cl_2 (10^{-5} M).

https://doi.org/10.1021/acs.inorgchem.3c00650
Inorg. Chem. 2023, 62, 8232−8248

Table 1. Selected Emission Data of Complexes 3, 4, and 5[a,b]

complex	medium (T/K)	$\lambda_{em(calc)}$ (nm)[c]	λ_{em} (nm)	τ (μs)[d]	Φ[e] (%)
3a	$PMMA_{5\%}$ (298)	539	**530**, 566	0.2 (4.2%), 4.0 (95.8%)	36
	CH_2Cl_2 (298)		**530**, 562	10.1	62
	CH_2Cl_2 (77)		**520**, 560, 696 (exc)	12.7 (45.5%), 5.1 (54.5%)	
	2-MeTHF (298)		**533**, 570	3.3	25
	2-MeTHF (77)		479, **523**, 559	11.5	
3c	$PMMA_{5\%}$ (298)	476	487, **524**, 550 (sh)	3.3 (14.1%), 9.7 (85.9%)	28
	CH_2Cl_2 (298)		**484**, 516, 548	5.0	20
	CH_2Cl_2 (77)		486, **526**, 556, 644 (exc)	15.4 (83.4%), 36.0 (16.6%)	
	2-MeTHF (298)		**486**, 522, 556	7.3	20
	2-MeTHF (77)		**480**, 506, 518, 548	24.9 (14.9%), 14.4 (85.1%)	
3d	$PMMA_{5\%}$ (298)	488	**488**, 521, 558	10.5	70
	CH_2Cl_2 (298)		**487**, 521, 559	11.9	16
	CH_2Cl_2 (77)		**486**, 524, 559	34.7 (53.5%), 17.4 (46.5%)	
	2-MeTHF (298)		**488**, 522, 560	20.1 (90.4%), 2.6 (9.6%)	35
	2-MeTHF (77)		**479**, 515, 551	36.2 (93.0%), 10.1 (7.0%)	
4a	$PMMA_{2\%}$ (298)	545	**529**, 559	0.5 (1.7%), 5.1 (98.3%)	22
	CH_2Cl_2 (298)		**530**, 560	10.2	23
	CH_2Cl_2 (77)		**521**, 559, 688 (exc)	46.0 (12.8%), 15.1 (87.2%)	
	2-MeTHF (298)		499, **531**, 567 (sh)	3.3 (89.8%), 0.3 (10.2%)	6
	2-MeTHF (77)		480, 490, **518**, 556	12.8	
4c	$PMMA_{2\%}$ (298)	487	**490**, 524, 563 (sh), 622 (exc)	4.2 (26.0%), 9.4 (74.0%)	26
	CH_2Cl_2 (298)		**488**, 522, 556	5.4	21
	CH_2Cl_2 (77)		**490**, 526, 568	21.0 (82.3%), 11.5 (17.7%)	
	2-MeTHF (298)		**486**, 520, 550	6.8	18
	2-MeTHF (77)		**480**, 516, 550	20.3 (41.1%), 13.3 (58.9%)	
4d	$PMMA_{5\%}$ (298)	491	**492**, 521, 563 (sh)	7.7	61
	CH_2Cl_2 (298)		493, **524**, 562 (sh)	11.0 (17.6%), 2.2 (82.4%)	7
	CH_2Cl_2 (77)		489, **520**, 559 (sh)	21.3 (29.8%), 6.9 (70.2%)	
	2-MeTHF (298)		**488**, 523, 559 (sh)	16.5 (19.7%), 10.0 (80.3%)	10
	2-MeTHF (77)		**478**, 514, 550	36.8 (86.5%), 18.0 (13.5%)	
5a	$PMMA_{5\%}$ (298)	524	**484**, 517, 556 (sh)	6.0	50
	CH_2Cl_2 (298)		**482**, 515, 554 (sh)	2.4	12
	CH_2Cl_2 (77)		**482**, 516, 555 (sh)	23.5 (44.1%), 10.4 (55.9%)	
	2-MeTHF (298)		**488**, 522, 559	4.7	12
	2-MeTHF (77)		**476**, 507, 546	19.5	
5c	$PMMA_{2\%}$ (298)	477	**487**, 524, 568, 609 (exc)	4.4 (16.1%), 12.1 (83.9%)	50
	CH_2Cl_2 (298)		**484**, 520, 558	7.1	23
	CH_2Cl_2 (77)		**488**, 526, 608 (exc)	27.6 (26.9%), 12.4 (73.1%)	
	2-MeTHF (298)		**486**, 522, 558	6.4	15
	2-MeTHF (77)		**480**, 508, 518, 552	30.3 (5.6%), 14.0 (94.4%)	
5d	$PMMA_{5\%}$ (298)	447	**484**, 516, 553	7.8	48
	CH_2Cl_2 (298)		**484**, 517, 555	11.7 (47.9%), 3.3 (52.1%)	5
	CH_2Cl_2 (77)		**482**, 517, 555 (sh)	32.0 (46.9%), 15.0 (53.1%)	
	2-MeTHF (298)		**483**, 517, 554	11.3 (23.1%), 4.1 (76.9%)	9
	2-MeTHF (77)		**478**, 511, 548 (sh)	53.3 (10.4%), 25.8 (89.6%)	

[a]Table 1 summarizes the data in Table S7. [b]Solutions 1×10^{-5} M. The most intense peak is in bold. (exc) λ_{em} excimer. [c]Computed values (SMD(CH_2Cl_2)-B3LYP-D3/def2-SVP) obtained from the differences in energy between the optimized triplet states T_1 and the singlet states S_0. [d]Relative amplitudes (%) are given in parentheses for biexponential decays. [e]Absolute quantum yield.

which has also been previously observed for *N,C,N*-pincer emitters of osmium(IV) and iridium(III). The rise in stability is ascribed to the approach of the pincer bite angles to the ideal values corresponding to the coordination polyhedron of the complex.[30]

The emission spectrum of **3a**, in CH_2Cl_2, at 298 K is independent of the emitter concentration, in the range $(1 \times 10^{-3})-(1 \times 10^{-6})$ M, and superimposable with that observed in $PMMA_{5\%}$ (Figure 7a). The lifetime increases from 0.8 to 11.9 μs, and the quantum yields from 0.05 to 0.60 as the emitter concentration decreases. This is indicative of self-quenching induced by ground-state aggregation.[31] Although excimer emission is not observed in the 700 nm region,[32] the rate of emission decay ($k_{obs} = 1/\tau$) fits well to the modified Stern–Volmer expression shown in eq 1, where k_q is the rate constant for the excimer formation, [Pt] is the emitter concentration, and k_0 ($=1/\tau_0$) is the rate of excited-state decay at infinite dilution. A plot of k_{obs} *versus* [Pt] (Figure S15) provides values for the self-quenching rate constant k_q and the intrinsic lifetime τ_0 of 1.2×10^9 M^{-1} s^{-1} and 11.5 μs, respectively.[33] At 77 K, the excimer life rises. As a consequence, at this temperature, the emission spectra of solutions, more concentrated than 1×10^{-6} M, clearly show the excimer broadband at about 700 nm, which increases its intensity as the emitter concentration also increases (Figure 7b). An analogous behavior was observed for the phenylacetylide derivative **4a**, which displays k_q and τ_0 values of 0.9×10^9 M^{-1} s^{-1} and 10.6 μs, respectively (see Figure S16). These values compare well with those reported for other emissive platinum complexes.[31,33a,34]

$$k_{obs} = k_0 + k_q[Pt] \quad (1)$$

https://doi.org/10.1021/acs.inorgchem.3c00650
Inorg. Chem. 2023, 62, 8232−8248

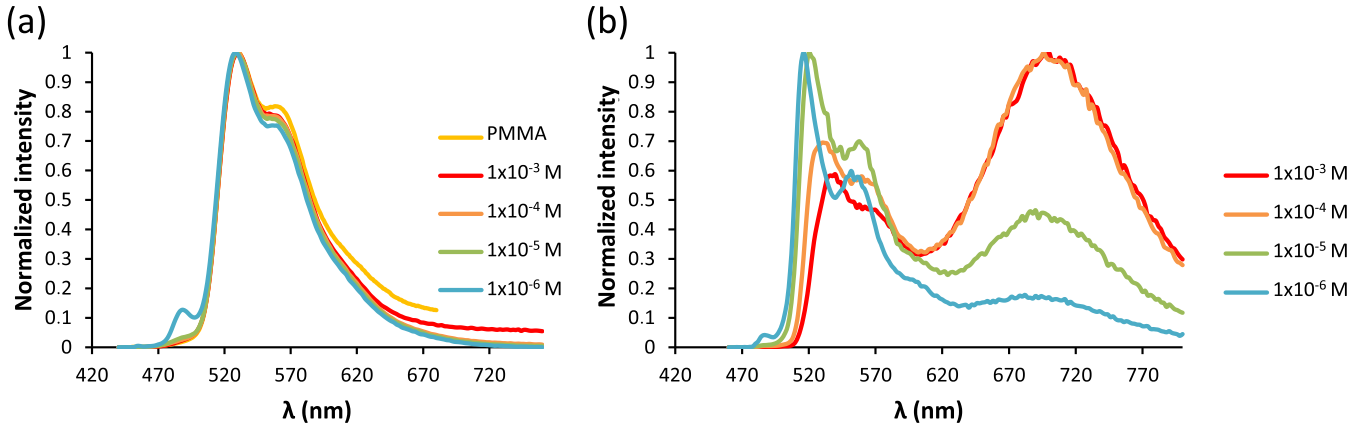

Figure 7. (a) Emission spectra of **3a** at 298 K in $PMMA_{5\%}$ and in dichloromethane at concentrations between 1×10^{-3} and 1×10^{-6} M. (b) Emission spectra of **3a** at 77 K in dichloromethane at concentrations between 1×10^{-3} and 1×10^{-6} M.

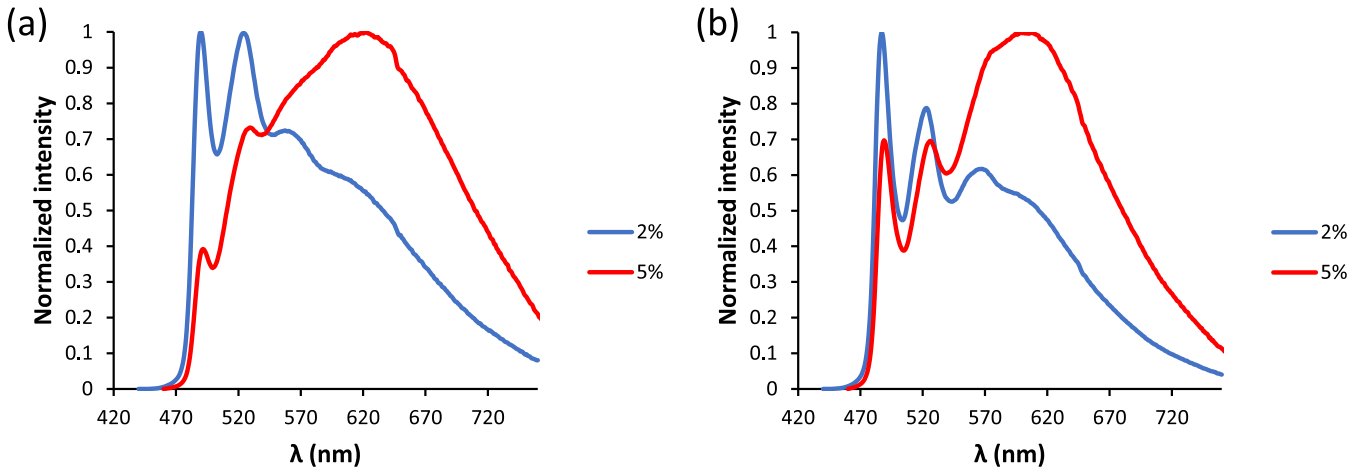

Figure 8. (a) Emission spectra of **4c** in $PMMA_{2\%}$ and $PMMA_{5\%}$. (b) Emission spectra of **5c** in $PMMA_{2\%}$ and $PMMA_{5\%}$.

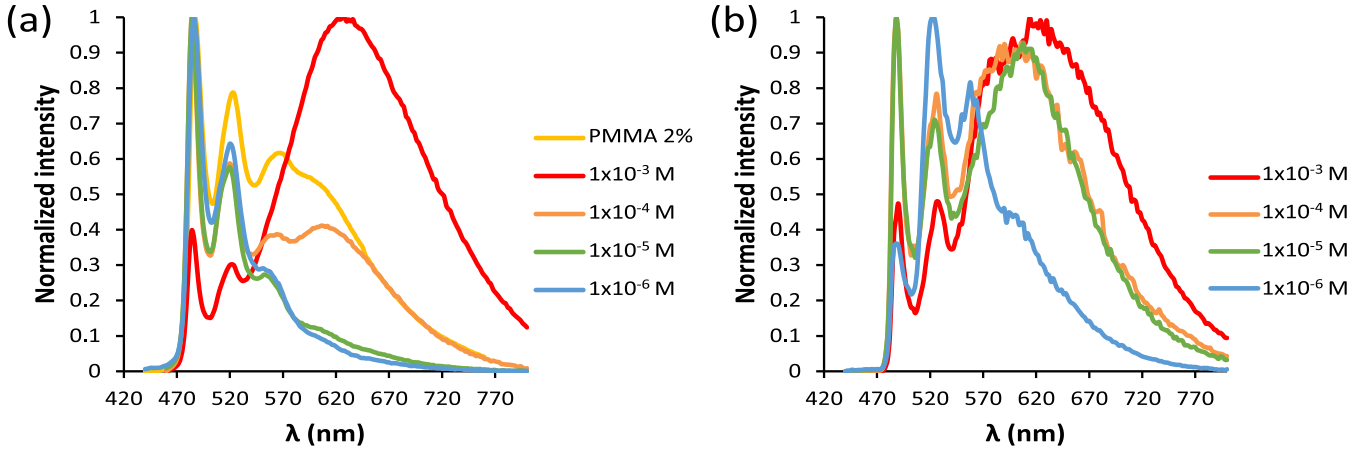

Figure 9. (a) Emission spectra of **5c** at 298 K in $PMMA_{2\%}$ and in dichloromethane at concentrations between 1×10^{-3} and 1×10^{-6} M. (b) Emission spectra of **5c** at 77 K in dichloromethane at concentrations between 1×10^{-3} and 1×10^{-6} M.

The solvent has a dramatic influence on the emission. For example, 2-MeTHF prevents self-quenching of **4a**, as shown in Figure S101, although changes in the relative intensity of the structured band peaks are observed as a consequence of variations in the emitter concentration. In addition, a mitigation of the quantum yield in $PMMA_{5\%}$ from 0.22 to a constant value of about 0.06 also occurs. The effect can be assigned to the different solvation abilities of the solvents and to a noticeable coordinating ability of the ether, which protects the unsaturated monomers.

There are significant differences between **4a** and its thermodynamic isomer **4d** in CH_2Cl_2. At 298 K, the structured emission of the latter consists of two peaks of similar intensity at 493 and 524 nm and a shoulder at 562 nm. As for **4a**, this shape is independent of the emitter concentration, in the range $(1 \times 10^{-3})-(1 \times 10^{-6}$ M) (Figures S63−S66) and

https://doi.org/10.1021/acs.inorgchem.3c00650
Inorg. Chem. 2023, 62, 8232−8248

superimposable with that obtained in $PMMA_{5\%}$ (Figures S62). However, in contrast to **4a**, the quantum yield for **4d** is constant in the concentration range and about ten times lower than in $PMMA_{5\%}$ (0.61 *versus* 0.07). Although the relative intensity of the peaks of the emission changes at 77 K, an excimer band is not observed. In this case, the significant mitigation of the quantum yields in CH_2Cl_2 appears to be due to a notable increase of the nonradiative rate constant in solution, which is an order of magnitude higher than that in $PMMA_{5\%}$ (5.1×10^4 *versus* 5.2×10^5 s^{-1} (1×10^{-3} M)).

Acetylido derivatives with a pyridine substituent **4c** and **5c** undergo self-quenching in the solid state (Figure 8).[35] Thus, the emission spectra in PMMA show an excimer broadband centered around 640 nm, in addition to the structured pattern of two peaks and a shoulder in the 490−570 nm region, which is characteristic of this class of complexes. As expected, the excimer emission significantly rises its intensity as the emitter concentration increases, being the most intense band at 5 wt %. The increase of the intensity of this band is accompanied by a decrease of the quantum yield of the emission, which diminishes from 0.26 to 0.15 for **4c** and from 0.50 to 0.35 for **5c** when the emitter concentration in the film increases from 2 to 5 wt %.

The behavior of emitter **5c** was also studied in solution, as a function of its concentration, in the range (1×10^{-3})−(1×10^{-6}) M, in CH_2Cl_2, at 298 and 77 K. Consistently with the behavior in the PMMA film, **5c** undergoes self-quenching in the solvent at both temperatures (Figure 9). As the emitter concentration rises, the intensity of the excimer broadband around 640 nm increases at the expense of peaks between 480 and 560 nm of the structured emission. At 298 K, the values obtained for the self-quenching rate constant k_q and the intrinsic lifetime τ_0 are 1.9×10^9 M^{-1} s^{-1} and 7.8 μs, respectively.

CONCLUSIONS

We describe an efficient methodology to prepare a new class of pincer complexes, with structures [5.5]- and [6.5]-Pt{κ^3-*N*,*C*,*N*′-[L]}X (X = Cl, RC≡C), built on 6-phenyl purines. The nucleobase skeleton provides an *N*,*C*-cyclometalated fragment, which was additionally functionalized with an amine, imine, or pyridine arm to afford the *N*,*C*,*N*′-pincer structure. The reactions were totally regioselective. Although the formation of [5.5]-bicycle compounds, bearing the purine bonded by *N*1, is kinetically favored for the amine arm, the [6.5]-bicycle isomers resulting from the *N*7 coordination of the purine are more stable in all of the cases. The combination of purine nucleoside pincer ligands with ethynylpurine nucleosides has furthermore allowed the preparation of novel heteroleptic bis-nucleoside compounds, which may be viewed as organometallic models of Pt-induced interstrand cross-link. The pincer compounds Pt{κ^3-*N*,*C*,*N*′-[L]}X (X = Cl, RC≡C) [Pt(N∧C∧N′)L] are square-planar complexes having the monodentate X ligand trans to the cyclometalated phenyl ring. In the solid state, noncovalent interactions between adjacent molecules have been observed by XRD. The complexes bearing an amine or pyridine arm are phosphorescent green emitters upon photoexcitation, displaying high quantum yields in PMMA and dichloromethane at low concentrations. At high concentrations, they undergo self-quenching favored by molecular aggregation of monomers through aromatic $\pi-\pi$ interactions that are reinforced by weak platinum−platinum interactions.

EXPERIMENTAL SECTION

General Methods. Unless stated otherwise, all of the reactions were carried out under an Ar atmosphere using anhydrous solvents. The reaction work-ups were performed in air. Commercially available reagents were used as received without further purification. 6-Chloro-9-ethylpurine,[36] 3-(2-pyridynyl)phenylboronic acid pinacol ester,[37] 6-ethynyl-9-ethylpurine,[38] and $PtCl_2(DMSO)_2$[39] were prepared according to reported protocols. ^1H and $^{13}C\{^1H\}$ NMR spectra were recorded at ambient temperature in $CDCl_3$ or CD_2Cl_2 on Bruker 500 or 300 MHz spectrometers. Chemical shifts are expressed in ppm and are referenced to residual solvent peaks. Through the experimental part, in the NMR spectra, the numbering of the purine ring system has been used to denote the positions *C*2 (*H*2) and *C*8 (*H*8) of the nucleobase. Fourier transform infrared (FT-IR) spectra (attenuated total reflection (ATR)) were recorded with solid or films (by slow evaporating $CHCl_3$ solutions of the compounds) on a Bruker Alpha spectrometer. Electrospray ionization-high-resolution mass spectrometry (ESI-HRMS) was performed on an Agilent 6500 accurate mass spectrometer with a Q-TOF analyzer. UV−visible spectra were registered on an Evolution 600 spectrophotometer. Steady-state photoluminescence spectra were recorded with either a Jobin-Yvon Horiba Fluorolog FL-3-11 Tau 3 spectrometer (PMMA films) or with a PicoQuant FluoTime 300 spectrometer (CH_2Cl_2 and 2-MeTHF solutions). Lifetime measurements were performed at the maximum emission wavelength of the complexes either on a Jobin-Yvon Horiba Fluorolog FL-3-11 Tau 3 spectrometer (PMMA films) or a PicoQuant FluoTime 300 spectrometer (CH_2Cl_2 and 2-MeTHF solutions). Data were fitted to either monoexponential or biexponential functions. Quantum yields were measured using the Hamamatsu Absolute PL Quantum Yield Measurement System C11347-11.

Computational Details. All calculations were performed at the DFT level using the B3LYP functional as implemented in Gaussian09[40] supplemented with the Grimme's dispersion correction D3[41] and the def2-SVP basis set.[42] All minima were verified to have no negative frequencies. The geometries were fully optimized in vacuo and in the appropriate solvent using the continuum SMD model.[43]

X-ray Diffraction Analyses. Crystals of **3a**·0.5($CHCl_3$), **3b**, **3c**·0.5(CH_2Cl_2), **3d**, **4b**, **4d**, and **5a** were analyzed by X-ray diffraction. A selection of crystal, measurement, and refinement data is given in Tables S1 and S2. Diffraction data were collected on an Oxford Diffraction Xcalibur Onyx Nova single-crystal diffractometer with Cu Kα radiation. Empirical absorption corrections were applied using the SCALE3 ABSPACK algorithm as implemented in CrysAlisPro RED.[44] The structures were solved with SIR-97.[45] Isotropic and full matrix anisotropic least-squares refinements were carried out using SHELXL.[46] All non-H atoms were refined anisotropically. H atoms were set in calculated positions and were refined riding on their parent atoms. The CH_2 and CH_3 groups of the fragment $CH_2N(CH_3)_2$ of **5a** were disordered over two positions with a 54:46 occupancy ratio, requiring restraints on its thermal parameters. The structure of **4d** was refined as a 2-component inversion twin. The high-resolution reflections $\bar{8}$ 3 4, $\bar{8}$ 2 3, and 5 21 2 were left out from the refinement of **3b** since their intensities were likely affected by some unresolved twinning, resulting in high *S* values. The low-resolution reflections $\bar{3}$ $\bar{3}$ 2 and 1 $\bar{7}$ 13 were left out from the refinement of **3d** since their intensities were likely affected by the beamstop, resulting in high *S* values. The WINGX program system[47] was used throughout the structure determinations. The molecular plots were made with MERCURY.[48]

Synthesis of **1**. 3-Formylphenylboronic acid (1.69 g, 8.7 mmol), $Pd(PPh_3)_4$ (388 mg, 0.34 mmol), and K_2CO_3 (1.20 g, 8.7 mmol) were added to a solution of 6-chloro-9-ethylpurine (1.22 g, 6.7 mmol) in 60 mL of toluene/ethanol (9:1). The mixture was refluxed under argon for 24 h. The solvent was removed under reduced pressure, and the crude residue was purified by flash SiO_2 chromatography (hexane/ethyl acetate, 1:1 to ethyl acetate) to yield **1** (white solid) (1.61 g, 95%). ^1H NMR (300 MHz, $CDCl_3$), δ (ppm): 10.2 (s, 1H, CHO), 9.33 (t, 1H, CH_{arom}), 9.12 (dt, 1H, CH_{arom}), 9.06 (s, 1H,

https://doi.org/10.1021/acs.inorgchem.3c00650
Inorg. Chem. 2023, 62, 8232−8248

CH2), 8.19 (s, 1H, CH8), 8.07 (dt, 1H, CH_{arom}), 7.74 (t, J = 7.5 Hz, 1H, CH_{arom}), 4.41 (q, 2H, J = 6.7 Hz, CH_2), 1.62 (t, 3H, J = 6.7 Hz, CH_3). ^{13}C NMR (75 MHz, $CDCl_3$), δ (ppm): 192.4 (CHO), 153.2 ($C_{quaternary}$), 152.5 (C2), 149.2 ($C_{quaternary}$), 144.4 (C8), 137.0 ($C_{quaternary}$), 135.7 (C_{arom}), 132.4 (C_{arom}), 131.5 ($C_{quaternary}$), 130.7 (C_{arom}), 129.6 (C_{arom}), 39.2 (CH_2), 15.6 (CH_3). IR (cm^{-1}): ν 3104, 2919, 1711, 1576. ESI-HRMS m/z: calcd for $C_{14}H_{13}N_4O$ $[M + H]^+$ 253.1083; found 253.1082.

Synthesis of ***2a***. $HNMe_2$·HCl (679 mg, 8.32 mmol), $Ti(O^iPr)_4$ (2.4 mL, 7.93 mmol), and Et_3N (2.5 mL) were added to a solution of **1** (1.00 g, 3.96 mmol) in 100 mL of ethanol, and the mixture was stirred at room temperature overnight. Then, $NaBH_3CN$ (374 mg, 5.94 mmol) was added, and the solution was stirred at room temperature for 24 h. The reaction mixture was quenched with water and extracted with DCM. The organic layers were dried over Na_2SO_4, and the solvent was evaporated under reduced pressure to yield **2a** (colorless oil) (1.09 g, 98%). ^1H NMR (300 MHz, $CDCl_3$), δ (ppm): 8.98 (s, 1H, CH2), 8.65−8.61 (m, 2H, CH_{arom}), 8.10 (s, 1H, CH8), 7.52−7.44 (m, 2H, CH_{arom}), 4.32 (q, J = 7.3 Hz, 2H, CH_2), 3.54 (s, 2H, NCH_2), 2.25 (s, 6H, $N(CH_3)_2$), 1.53 (t, J = 7.3 Hz, 3H, CH_3). ^{13}C NMR (75 MHz, $CDCl_3$), δ (ppm): 154.8 ($C_{quaternary}$), 152.3 ($C_{quaternary}$), 152.3 (C2), 143.9 (C8), 139.2 ($C_{quaternary}$), 135.8 ($C_{quaternary}$), 131.8 (C_{arom}), 131.2 ($C_{quaternary}$), 130.4 (C_{arom}), 128.9 (C_{arom}), 128.7 ($C_{quaternary}$), 64.3 (NCH_2), 45.3 ($N(CH_3)_2$), 39.0 (CH_2), 15.6 (CH_3). IR (cm^{-1}): 2923, 2852, 1572, 1498. ESI-HRMS m/z: calcd for $C_{16}H_{20}N_5$ $[M + H]^+$ 282.1713, found 282.1718.

Synthesis of ***2b***. *p*-Anisidine (244 mg, 1.98 mmol) and $MgSO_4$ (10% w/w) were added to a solution of **1** (500 mg, 1.98 mmol) in 10 mL of DCM. The mixture was stirred at room temperature for 24 h. Then, $MgSO_4$ was filtered off, and the solvent was removed under reduced pressure to yield **2b** (white solid) (687.5 mg, 97%, EtOH). ^1H NMR (300 MHz, $CDCl_3$), δ (ppm): 9.19 (t, J = 1.7 Hz, 1H, CH_{arom}), 9.06 (s, 1H, CH2), 8.93 (dt, J = 7.8, 1.5 Hz, 1H, CH_{arom}), 8.66 (s, 1H, CH═N), 8.19 (m, 1H, CH_{arom}), 8.17 (s, 1H, CH8), 7.68 (t, J = 7.8 Hz, 1H, CH_{arom}), 7.29 (d, J = 8.9 Hz, 2H, CH_{arom}), 6.95 (d, J = 8.9 Hz, 2H, CH_{arom}), 4.40 (q, J = 7.3, 2H, CH_2), 3.85 (s, 3H, CH_3), 1.62 (t, J = 7.3, 3H, CH_3). ^{13}C NMR (75 MHz, $CDCl_3$), δ (ppm): 158.5 ($C_{quaternary}$), 158.2 (CH═N), 154.2 ($C_{quaternary}$), 152.6 ($C_{quaternary}$), 152.5 (C2), 145.0 ($C_{quaternary}$), 144.2 (C8), 137.2 ($C_{quaternary}$), 136.5 ($C_{quaternary}$), 132.5 (C_{arom}), 131.5 ($C_{quaternary}$), 130.9 (C_{arom}), 130.0 (C_{arom}), 129.3 (C_{arom}), 122.5 (C_{arom}), 114.5 (C_{arom}), 55.6 (OCH_3), 39.2 (CH_2), 15.6 (CH_3). IR (film) ν (cm^{-1}): 2923, 1618, 1572, 1498, 1235. ESI-HRMS m/z: calcd for $C_{21}H_{20}N_5O1$ $[M + H]^+$, 358.1662; found 358.1660.

Synthesis of ***2c***. To a solution of 6-chloro-9-ethylpurine (174 mg, 0.95 mmol) in 15 mL of a mixture of toluene and ethanol (9:1) were added 3-(2-pyridynyl)phenylboronic acid pinacol ester (348 mg, 1.23 mmol), $Pd(PPh_3)_4$ (79 mg, 0.07 mmol), and K_2CO_3 (246 mg, 1.8 mmol). The mixture was refluxed under argon for 24 h. The solvent was removed under reduced pressure, and the residue was purified by flash SiO_2 chromatography (hexane/ethyl acetate, 1:1 to ethyl acetate) to yield **2c** (white solid) (155 mg, 54%). ^1H NMR (300 MHz, $CDCl_3$), δ (ppm): 9.39 (br s, 1H, CH_{arom}), 9.04 (s, 1H, CH2), 8.89 (d, J = 6.8 Hz, 1H, CH_{arom}), 8.74 (d, J = 4.4 Hz, 1H, CH_{arom}), 8.23 (d, J = 6.6 Hz, 1H, CH_{arom}), 8.16 (s, 1H, CH8), 7.92 (d, J = 8.93 Hz, 1H, CH_{arom}), 7.80 (td, J = 7.7 and 1.7 Hz, 1H, CH_{arom}), 7.68 (t, J = 7.8 Hz, 1H, CH_{arom}), 7.29−7.25 (m, 1H, CH_{arom}), 4.37 (q, J = 7.3 Hz, 2H, CH_2), 1.59 (t, J = 7.3 Hz, 3H, CH_3). ^{13}C NMR (75 MHz, $CDCl_3$), δ (ppm): 157.0 ($C_{quaternary}$), 154.4 ($C_{quaternary}$), 152.5 ($C_{quaternary}$), 152.3 (C2), 149.5 (C_{arom}), 144.0 (C8), 139.5 (C), 137.1 (C_{arom}), 136.3 ($C_{quaternary}$), 132.1 ($C_{quaternary}$), 130.6 (CH_{arom}), 129.5 (CH_{arom}), 129.3 (CH_{arom}), 128.2 (CH_{arom}), 122.4 (CH_{arom}), 121.0 (CH_{arom}), 39.0 (CH_2), 15.4 (CH_3). IR (film) ν (cm^{-1}): 2982, 1565, 1315. ESI-HRMS m/z: calcd for $C_{18}H_{16}N_5$, $[M + H]^+$, 302.1400; found 302.1400.

Synthesis of ***3a***. Compound **2a** (213 mg, 0.756 mmol) was added to a suspension of K_2PtCl_4 (314 mg, 0.756 mmol) in 15 mL of AcOH. The mixture was refluxed under argon for 3 days. The solvent was removed under reduced pressure, and the residue was purified by flash SiO_2 chromatography (DCM/ethyl acetate 1:1 to 1:9) to yield **3a** (bright yellow solid) (215 mg, 56%). ^1H NMR (500 MHz, $CDCl_3$), δ (ppm): 9.40 (s, $J(^1H-^{195}Pt)$ = 11.5 Hz, 1H, CH2), 8.16 (m, 1H, CH_{arom}), 8.14 (s, 1H, CH8), 7.12 (t, J = 7.6 Hz, 1H, CH_{arom}), 6.99 (d, J = 7.0 Hz, 1H, CH_{arom}), 4.37 (q, J = 7.3 Hz, 2H, CH_2), 4.25 (s, $J(^1H-^{195}Pt)$ = 17.0 Hz, 2H, NCH_2), 3.25 (s, $J(^1H-^{195}Pt)$ = 15.8 Hz, 6H, $N(CH_3)$), 1.60 (t, J = 7.4 Hz, 3H, CH_3). ^{13}C NMR (126 MHz, $CDCl_3$), δ (ppm): 165.7 (C−Pt), 157.0 ($C_{quaternary}$), 154.3 (C2), 152.5 ($C_{quaternary}$), 145.9 (C8), 143.4 ($C_{quaternary}$), 138.4 ($C_{quaternary}$), 129.2 ($C_{quaternary}$), 127.7 (C_{arom}), 125.1 (C_{arom}), 123.2 (C_{arom}), 77.9 (NCH_2), 54.2 ($N(CH_3)_2$), 39.2 (CH_2), 15.2 (CH_3). IR (film) ν (cm^{-1}): 2928, 1747, 1577, 1499, 1457. ESI-HRMS m/z: calcd for $C_{16}H_{18}N_5Pt$, $[M-Cl]^+$, 475.1206; found 475.1209.

Synthesis of ***3b***. As for **3a**, from K_2PtCl_4 (232 mg, 0.56 mmol) in 15 mL of AcOH and **2b** (200 mg, 0.56 mmol). The solvent was removed under reduced pressure, and the residue was purified by flash SiO_2 chromatography (DCM/ethyl acetate, 2:8) to yield **3b** (bright yellow solid) (151 mg, 46%). ^1H NMR (300 MHz, CD_2Cl_2), δ (ppm): 9.29 (s, $J(^1H-^{195}Pt)$ = 11.2 Hz, 1H, CH8), 8.99 (s, 1H, CH2), 8.54 (dd, J = 7.9, 1.2 Hz, 1H, CH_{arom}), 8.33 (s, $J(^1H-^{195}Pt)$ = 58.6 Hz, 1H, CH═N), 7.65 (dd, J = 6.7, 1.3 Hz, 1H, CH_{arom}), 7.45 (d, J = 8.8 Hz, 2H, CH_{arom}), 7.37 (t, J = 8.2 Hz, 1H, CH_{arom}), 6.96 (d, J = 8.8 Hz, 2H, CH_{arom}), 4.39 (q, J = 7.4 Hz, 2H, CH_2), 3.87 (s, 3H, OCH_3), 1.58 (t, J = 7.5 Hz, 3H, CH_3). ^{13}C NMR (75 MHz, CD_2Cl_2), δ (ppm): 178.1 (C═N), 159.8 (C−Pt), 155.3 ($C_{quaternary}$), 154.0 (C2), 150.7 ($C_{quaternary}$), 150.0 ($C_{quaternary}$), 147.9 ($C_{quaternary}$), 145.8 (C8), 142.9 ($C_{quaternary}$), 132.5 (C_{arom}), 130.1 (C_{arom}), 128.7 ($C_{quaternary}$), 126.0 (C_{arom}), 124.3 (C_{arom}), 121.7 ($C_{quaternary}$), 113.6 (C_{arom}), 56.1 (OCH_3), 41.2 (CH_2), 15.3 (CH_3). IR (film) ν (cm^{-1}): 2965, 1607, 1507. ESI-HRMS m/z: calcd for $C_{21}H_{18}N_5OPt$, $[M-Cl]^+$, 551.1155; found 551.1158.

Synthesis of ***3c***. As for **3a**, from K_2PtCl_4 (276 mg, 0.66 mmol) in 15 mL of AcOH and **2c** (200 mg, 0.66 mmol). The mixture was refluxed under argon for 4 days. The product precipitated after cooling. The solid was filtered and washed with cold MeOH and diethyl ether to yield **3c** (bright yellow solid) (183 mg, 52%). ^1H NMR (500 MHz, CD_2Cl_2), δ (ppm): 9.62 (d, J = 5.9 Hz, $J(^1H-^{195}Pt)$ = 15.9 Hz, 1H, CH_{arom}), 9.37 (s, $J(^1H-^{195}Pt)$ = 14.2 Hz, 1H, CH8), 8.98 (s, 1H, CH2), 8.61 (d, J = 10.0 Hz, 1H, CH_{arom}), 7.92 (t, J = 10.0 Hz, 1H, CH_{arom}), 7.77 (d, J = 8.3 Hz, 1H, CH_{arom}), 7.71 (d, J = 7.7 Hz, 1H, CH_{arom}), 7.36 (t, J = 6.2 Hz, 1H, CH_{arom}), 7.25 (t, J = 6.6 Hz, 1H, CH_{arom}), 4.45 (q, J = 7.4 Hz, 2H, CH_2), 1.64 (t, J = 7.4 Hz, 3H, CH_3). ^{13}C NMR (126 MHz, CD_2Cl_2), δ (ppm): 166.6 ($C_{quaternary}$), 156.1 (C−Pt), 154.2 (C2), 150.9 (C_{arom}), 150.7 ($C_{quaternary}$), 146.9 ($C_{quaternary}$), 146.4 ($C_{quaternary}$), 146.2 (C8), 139.4 (C_{arom}), 129.3 ($C_{quaternary}$), 128.5 (C_{arom}), 127.4 (C_{arom}), 124.6 (C_{arom}), 123.2 (C_{arom}), 121.9 ($C_{quaternary}$), 119.4 ($C_{quaternary}$), 41.1 (CH_2), 15.5 (CH_3). IR (film) ν (cm^{-1}): 2963, 1607, 1581. ESI-HRMS m/z: calcd for $C_{18}H_{14}N_5Pt$, $[M - Cl]^+$, 495.0893; found, 495.0883.

Synthesis of ***3d***. A solution of **3a** (200 mg, 0.39 mmol) in 5 mL of dry toluene was heated in a sealed tube at 200 °C for 5 days. After the removal of the solvent under vacuum, the crude product was purified by flash SiO_2 chromatography (DCM/ethyl acetate, 2:8) to yield **3d** (yellow solid, 197 mg, 99%). ^1H NMR (500 MHz, CD_2Cl_2), δ (ppm): 9.14 (s, $J(^1H-^{195}Pt)$ = 10.5 Hz, 1H, CH8), 8.99 (s, 1H, CH2), 8.42−8.39 (m, 1H, CH_{arom}), 7.25−7.21 (m, 2H, CH_{arom}), 4.37 (q, J = 7.3 Hz, 2H, CH_2), 4.05 (s, $J(^1H-^{195}Pt)$ = 19.7 Hz, 2H, CH_2N), 3.10 (s, $J(^1H-^{195}Pt)$ = 16.2 Hz, 6H, $N(CH_3)_2$), 1.57 (t, J = 7.3 Hz, 3H, CH_3). ^{13}C NMR (126 MHz, CD_2Cl_2), δ (ppm): 156.6 (C−Pt), 154.3 (C2), 150.6 ($C_{quaternary}$), 150.3 ($C_{quaternary}$), 145.6 (C8), 141.5 ($C_{quaternary}$), 129.2 ($C_{quaternary}$), 124.9 (C_{arom}), 124.3 (C_{arom}), 124.0 (C_{arom}), 121.7 ($C_{quaternary}$), 76.1 (CH_2N), 54.2 ($N(CH_3)_2$), 40.9 (CH_2), 15.5 (CH_3). IR (film) ν (cm^{-1}): 2899, 1605, 1411, 1202. ESI-HRMS m/z: calcd for $C_{16}H_{18}N_5Pt$, $[M - Cl]^+$, 475.1206; found 475.1198.

Synthesis ***4a***. A mixture of phenylacetylene (15 mg, 0.15 mmol) and NaOH (6.0 mg, 0.15 mmol) in 5 mL of MeOH was stirred for 30 min at rt. Then, **3a** (50 mg, 0.1 mmol) was added to the reaction mixture and further stirred for 24 h. After filtration, the resulting solid was washed with cold methanol and diethyl ether to yield **4a** (bright yellow solid) (43 mg, 76%). ^1H NMR (500 MHz, CD_2Cl_2), δ (ppm): 9.54 (s, $J(^1H-^{195}Pt)$ = 13.9 Hz, 1H, CH2), 8.25 (dd, J = 6.1, 2.4 Hz,

https://doi.org/10.1021/acs.inorgchem.3c00650
Inorg. Chem. 2023, 62, 8232−8248

1H, CH_{arom}), 8.16, (s, 1H, CH8), 7.43−7.40 (m, 2H, CH_{arom}), 7.27−7.22 (m, 2H, CH_{arom}), 7.16−7.10 (m, 3H, CH_{arom}), 4.41−4.27 (m, 4H, CH_2 and CH_2N), 3.36 (s, $J(^1H-^{195}Pt)$ = 21.4 Hz, 6H, $N(CH_3)_2$), 1.57 (t, J = 7.3 Hz, 3H, CH_3). ^{13}C NMR (126 MHz, CD_2Cl_2), δ (ppm): 177.2 (C−Pt), 168.5 (C−Pt), 157.7 (C2), 152.9 ($C_{quaternary}$), 147.0 ($C_{quaternary}$), 146.7 (C8), 141.4 ($C_{quaternary}$), 136.5 ($C_{quaternary}$), 131.9 (C_{arom}), 129.5 ($C_{quaternary}$), 128.5 (C_{arom}), 127.9 (C_{arom}), 125.4 (C_{arom}), 125.2 (C_{arom}), 123.9 (C_{arom}), 123.7 ($C_{quaternary}$), 110.5 ($C_{quaternary}$), 80.8 (CH_2N), 56.3 ($N(CH_3)_2$), 39.8 (CH_2), 15.6 (CH_3). IR (film) ν (cm^{-1}): 2926, 2355, 2080, 1602, 1575. ESI-HRMS m/z: calcd for $C_{24}H_{24}N_5Pt$, $[M + H]^+$, 577.1676; found 577.1681.

Synthesis of ***4b***. As for **4a**, from phenylacetylene (13 mg, 0.13 mmol), NaOH (5.1 mg, 0.13 mmol), and **3b** (50 mg, 0.09 mmol). Complex **4b** was obtained as a bright yellow solid (40 mg, 72%). ^1H NMR (500 MHz, CD_2Cl_2), δ (ppm): 9.32 (s, $J(^1H-^{195}Pt)$ = 13.4 Hz, 1H, CH8), 8.96 (s, 1H, CH2), 8.60 (dd, J = 7.9, 13 Hz, 1H, CH_{arom}), 8.48 (s, $J(^1H-^{195}Pt)$ = 53.0 Hz, 1H, CH═N), 7.72 (dd, J = 7.3, 1.0 Hz, 1H, CH_{arom}), 7.68 (d, J = 8.8 Hz, 2H, CH_{arom}), 7.38 (t, J = 7.5 Hz, 1H, CH_{arom}), 7.22−7.19 (m, 4H, CH_{arom}), 7.16−7.12 (m, 1H, CH_{arom}), 6.95 (d, J = 8.8 Hz, 2H, CH_{arom}), 4.35 (q, J = 7.4 Hz, 2H, CH_2), 3.85 (s, 3H, OCH_3), 1.55 (t, J = 7.3 Hz, 3H, CH_3). ^{13}C NMR (126 MHz, CD_2Cl_2), δ (ppm): 179.4 (C═N), 171.2 (C−Pt), 159.8 (C−Pt), 157.2 ($C_{quaternary}$), 153.9 (C2), 150.6 ($C_{quaternary}$), 149.9 ($C_{quaternary}$), 148.1 (C8), 144.8 ($C_{quaternary}$), 131.8 (C_{arom}), 131.7 (C_{arom}), 130.7 ($C_{quaternary}$), 129.4 (C_{arom}), 129.0 ($C_{quaternary}$), 128.5 (C_{arom}), 126.1 (C_{arom}), 125.9 ($C_{quaternary}$), 125.7 (C_{arom}), 124.5 (C_{arom}), 122.0 ($C_{quaternary}$), 113.5 (C_{arom}), 108.5 ($C_{quaternary}$), 56.1 (OCH_3), 41.0 (CH_2), 15.1 (CH_3). IR (film) ν (cm^{-1}): 2922, 2095, 1603, 1503, 1247. ESI-HRMS m/z: calcd for $C_{29}H_{24}N_5OPt$, $[M + H]^+$, 653.1625; found, 653.1621.

Synthesis of ***4c***. As for **4b**, from phenylacetylene (12 mg, 0.13 mmol), NaOH (5.1 mg, 0.13 mmol), and **3c** (40 mg, 0.08 mmol). Complex **4c** was obtained as a bright orange solid (35 mg, 78%). ^1H NMR (500 MHz, CD_2Cl_2), δ (ppm): 9.93 (dd, J = 6.2 Hz, $J(^1H-^{195}Pt)$ = 23.5 Hz, 1H, CH_{arom}), 9.36 (s, $J(^1H-^{195}Pt)$ = 13.5 Hz, 1H, CH8), 9.04 (s, 1H, CH2), 8.78 (d, J = 7.8, 1H, CH_{arom}), 7.95−7.91 (m, 1H, CH_{arom}), 7.83 (d, J = 7.2 Hz, 2H, CH_{arom}), 7.55 (dd, J = 8.1, 1.4 Hz, 2H, CH_{arom}), 7.42 (t, J = 7.7 Hz, 1H, CH_{arom}), 7.32 (t, J = 6.2 Hz, 1H, CH_{arom}), 7.24−7.20 (m, 2H, CH_{arom}), 4.45 (q, J = 7.4 Hz, 2H, CH_2), 1.63 (t, J = 7.3 Hz, 3H, CH_3). ^{13}C NMR (126 MHz, CD_2Cl_2), δ (ppm): 168.7 (C−Pt), 167.0 (C−Pt), 158.2 ($C_{quaternary}$), 154.6 (C_{arom}), 154.2 (C2), 150.6 ($C_{quaternary}$), 148.7 ($C_{quaternary}$), 148.5 (C8), 139.9 (C_{arom}), 131.9 (C_{arom}), 131.4 ($C_{quaternary}$), 129.0 (C_{arom}), 128.7 (C_{arom}), 128.0 (C_{arom}), 127.1 ($C_{quaternary}$), 126.4 ($C_{quaternary}$), 126.0 (C_{arom}), 124.9 (C_{arom}), 123.7 (C_{arom}), 122.0 ($C_{quaternary}$), 119.7 (C_{arom}), 106.6 ($C_{quaternary}$), 40.9 (CH_2), 15.4 (CH_3). IR (film) ν (cm^{-1}): 2086, 1605, 1480. ESI-HRMS m/z: calcd for $C_{26}H_{20}N_5Pt$, $[M + H]^+$, 597.1363; found, 597.1345.

Synthesis of ***4d***. As for **4b**, from phenylacetylene (11 mg, 0.10 mmol), NaOH (3 mg, 0.10 mmol), and **3d** (35 mg, 0.08 mmol). Complex **4d** was obtained as a yellow solid, (21 mg, 53%). ^1H NMR (500 MHz, CD_2Cl_2), δ (ppm): 9.16 (s, $J(^1H-^{195}Pt)$ = 15.3 Hz, 1H, CH8), 9.03 (s, 1H, CH2), 8.54 (d, J = 6.4 Hz, 1H, CH_{arom}), 7.45−7.41 (m, 2H, CH_{arom}), 7.35−7.24 (m, 4H, CH_{arom}), 7.20−7.14 (m, 1H, CH_{arom}), 4.40 (q, J = 7.3 Hz, 2H, CH_2), 4.16 (s, $J(^1H-^{195}Pt)$ = 19.0 Hz, 2H, NCH_2), 3.30 (s, $J(^1H-^{195}Pt)$ = 20.8 Hz, 6H, $N(CH_3)_2$), 1.59 (t, J = 7.3 Hz, 3H, CH_3). ^{13}C NMR (126 MHz, CD_2Cl_2), δ (ppm): 164.7 (C−Pt), 158.7 (C−Pt), 154.2 (C2), 152.2 ($C_{quaternary}$), 150.6 ($C_{quaternary}$), 147.9 (C8), 131.8 (C_{arom}), 131.4 ($C_{quaternary}$), 129.2 ($C_{quaternary}$), 128.6 (C_{arom}), 125.8 ($C_{quaternary}$), 125.7 (C_{arom}), 124.4 (C_{arom}), 123.4 (C_{arom}), 121.9 ($C_{quaternary}$), 105.2 ($C_{quaternary}$), 78.1 (NCH_2), 56.0 ($N(CH_3)_2$), 40.7 (CH_2), 15.5 (CH_3). IR (film) ν (cm^{-1}): 2915, 2088, 1600, 1440, 1200. ESI-HRMS m/z: calcd for $C_{24}H_{24}N_5Pt$, $[M + H]^+$, 577.1676; found, 577.1679.

Synthesis of ***5a***. As for **4a**, from 9-ethyl-6-ethynylpurine (25 mg, 0.15 mmol), NaOH (5.9 mg, 0.15 mmol), and **3a** (50 mg, 0.1 mmol). Complex **5a** was obtained as a bright yellow solid (41 mg, 65%). ^1H NMR (500 MHz, $CDCl_3$), δ (ppm): 9.74 (s, $J(^1H-^{195}Pt)$ = 12.7 Hz, 1H, CH2), 8.84 (s, 1H, CH2′), 8.28 (dd, J = 7.7, 1.5 Hz, 1H, CH_{arom}), 8.14 (s, 1H, CH8), 8.04 (s, 1H, CH8′), 7.18−7.10 (m, 2H, CH_{arom}), 4.43−4.28 (m, 6H, $2CH_2$ and NCH_2), 3.46 (s, $J(^1H-^{195}Pt)$ = 20.4 Hz, 6H, $N(CH_3)_2$), 1.60−1.54 (m, 6H, $2CH_3$). ^{13}C NMR (126 MHz, $CDCl_3$), δ (ppm): 176.0 (C−Pt), 168.1 (C−Pt), 157.9 (C2), 155.6 ($C_{quaternary}$), 152.7 (C2′), 152.4 ($C_{quaternary}$), 150.7 ($C_{quaternary}$), 146.4 ($C_{quaternary}$), 145.9 (C8), 145.4 ($C_{quaternary}$), 142.9 (C8′), 141.4 ($C_{quaternary}$), 135.0 ($C_{quaternary}$), 129.8 ($C_{quaternary}$), 127.8 (C_{arom}), 124.9 (C_{arom}), 124.1 (C_{arom}), 106.4 ($C_{quaternary}$), 80.4 (NCH_2), 56.3 ($N(CH_3)_2$), 39.4 (CH_2), 38.9 (CH_2), 15.6 (CH_3), 15.4 (CH_3). IR (film) ν (cm^{-1}): 2936, 2078, 1603, 1560, 1208. ESI-HRMS m/z: calcd for $C_{25}H_{26}N_9Pt$, $[M + H]^+$, 647.1955; found, 647.1951.

Synthesis of ***5b***. As for **4a**, from 9-ethyl-6-ethynylpurine (22 mg, 0.13 mmol), NaOH (5.1 mg, 0.13 mmol), and **3b** (50 mg, 0.09 mmol). Complex **5b** was obtained as a bright orange solid (49 mg, 79%). ^1H NMR (500 MHz, CD_2Cl_2), δ (ppm): 10.5 (s, 1H, $J(^1H-^{195}Pt)$ = 12.7 Hz, C8), 8.83 (s, 1H, C2), 8.66 (s, 1H, C2′), 8.48 (dd, 1H, J = 7.9, 1.2 Hz, CH_{arom}), 8.42 (s, 1H, $J(^1H-^{195}Pt)$ = 53.4 Hz, CH═N), 7.72 (d, 2H, J = 8.7 Hz, CH_{arom}), 7.71 (s, 1H, C8′), 7.66 (dd, 1H, J = 7.3 and 1.2 Hz, CH_{arom}), 7.35 (t, 1H, J = 7.6 Hz, CH_{arom}), 6.94 (d, 2H, J = 8.9 Hz, CH_{arom}), 4.45 (q, 2H, J = 7.4 Hz, CH_2), 4.15 (q, 2H, J = 7.3 Hz, CH_2), 3.84 (s, 3H, CH_3), 1.52 (t, 3H, J = 7.4 Hz, CH_3), 1.49 (t, 3H, J = 7.3 Hz, CH_3). ^{13}C NMR (126 MHz, CD_2Cl_2), δ (ppm): 179.2 (C═N), 169.6 (C−Pt), 159.8 (C−Pt), 156.4 ($C_{quaternary}$), 153.4 (C2), 152.7 (C2), 150.8, (C8), 150.6 ($C_{quaternary}$), 150.6 ($C_{quaternary}$), 149.8 ($C_{quaternary}$), 145.2 ($C_{quaternary}$), 144.9 ($C_{quaternary}$), 144.6 ($C_{quaternary}$), 142.8 (C8), 135.6 ($C_{quaternary}$), 131.6 (C_{arom}), 130.8 ($C_{quaternary}$), 129.3 (C_{arom}), 126.1 (C_{arom}), 124.8 (C_{arom}), 122.0 ($C_{quaternary}$), 113.6 (C_{arom}), 104.9 ($C_{quaternary}$), 56.1 (OCH_3), 40.8 (CH_2), 39.3 (CH_2), 15.6 (CH_3), 15.5 (CH_3). IR (film) ν (cm^{-1}): 3012, 2079, 1602, 1572, 1208. ESI-HRMS m/z: calcd for $C_{30}H_{26}N_9OPt$, $[M + H]^+$, 723.1904; found, 723.1882.

Synthesis of ***5c***. As for **4a**, from 9-ethyl-6-ethynylpurine (12 mg, 0.13 mmol), NaOH (5.1 mg, 0.13 mmol), and **3c** (40 mg, 0.08 mmol). Complex **5c** was obtained as a bright orange solid (35 mg, 78%). ^1H NMR (500 MHz, CD_2Cl_2), δ (ppm): 10.6 (s, $J(^1H-^{195}Pt)$ = 14.8 Hz, 1H, CH8), 9.86 (d, J = 6.3 Hz, $J(^1H-^{195}Pt)$ = 24.6 Hz, 1H, CH_{arom}), 8.97 (s, 1H, CH2), 8.81 (s, 1H, CH2′), 8.73 (d, J = 7.4 Hz, 1H, CH_{arom}), 8.01 (s, 1H, CH8′), 7.92 (t, J = 7.4 Hz, 1H, CH_{arom}), 7.80 (d, J = 9.8 Hz, 2H, CH_{arom}), 7.40 (t, J = 7.4, 1H, CH_{arom}), 7.24 (t, J = 7.4 Hz, 1H, CH_{arom}), 4.61 (q, J = 7.1 Hz, 2H, CH_2), 4.32 (q, J = 7.6 Hz, 2H, CH_2), 1.73 (t, J = 7.1 Hz, 3H, CH_3), 1.58 (t, J = 7.4 Hz, 3H, CH_3). ^{13}C NMR (126 MHz, CD_2Cl_2), δ (ppm): 170.1 (C−Pt), 160.3 (C_{arom}), 156.8 (C−Pt), 153.8 (C2), 153.8 (C2), 153.1, (C8), 151.2 ($C_{quaternary}$), 151.0 ($C_{quaternary}$), 150.2 ($C_{quaternary}$), 145.6 ($C_{quaternary}$), 154.3 ($C_{quaternary}$), 145.0 ($C_{quaternary}$), 143.3 (C8), 136.0 ($C_{quaternary}$), 131.2 (C_{arom}), 129.7 ($C_{quaternary}$), 126.5 (C_{arom}), 125.2 (C_{arom}), 122.4 (C_{arom}), 105.4 ($C_{quaternary}$), 41.3 (CH_2), 39.8 (CH_2), 16.1 (CH_3), 15.9 (CH_3). IR (film) ν (cm^{-1}): 2964, 2366, 2086, 1563. ESI-HRMS m/z: calcd for $C_{27}H_{22}N_9Pt$, $[M + H]^+$, 667.1642; found, 667.1623.

Synthesis of ***5d***. As for **4a**, from 9-ethyl-6-ethynylpurine (15.2 mg, 0.09 mmol), NaOH (3.5 mg, 0.09 mmol), and **3d** (30 mg, 0.06 mmol). Complex **5d** was obtained as a yellow solid (25.8 mg, 68%). ^1H NMR (500 MHz, CD_2Cl_2), δ (ppm): 10.4 (s, $J(^1H-^{195}Pt)$ = 13.3 Hz, 1H, CH8), 8.99 (s, 1H, CH2), 8.88 (s, 1H, CH_2'), 8.53 (dd, J = 6.6, 2.6 Hz, 1H, CH_{arom}), 8.01 (s, 1H, CH8′), 7.33−7.24 (m, 2H, CH_{arom}), 4.55 (q, J = 7.3 Hz, 2H, CH_2), 4.36 (q, J = 7.3 Hz, 2H, CH_2), 4.17 (s, $J(^1H-^{195}Pt)$ = 18.6 Hz, 2H, NCH_2), 3.39 (s, $J(^1H-^{195}Pt)$ = 20.1 Hz, 6H, $N(CH_3)_2$), 1.70 (t, J = 7.3 Hz, 3H, CH_3), 1.62 (t, J = 7.3 Hz, 3H, CH_3). ^{13}C NMR (126 MHz, CD_2Cl_2), δ (ppm): 163.7 (C−Pt), 158.2 (C−Pt), 154.0 (C2), 153.2 (C2), 152.4 ($C_{quaternary}$), 151.1 ($C_{quaternary}$), 150.6 ($C_{quaternary}$), 149.8 (C8), 145.9 ($C_{quaternary}$), 145.6 ($C_{quaternary}$), 143.2 (C8), 136.6 ($C_{quaternary}$), 131.7 ($C_{quaternary}$), 124.8 (C_{arom}), 123.4 (C_{arom}), 123.3 (C_{arom}), 121.9 ($C_{quaternary}$), 102.2 ($C_{quaternary}$), 77.8 (NCH_2), 56.3 ($N(CH_3)_2$), 40.6 (CH_2), 39.4 (CH_2), 15.7 (CH_3). IR (film) ν (cm^{-1}): 2927, 2083, 1604, 1572, 1210. ESI-HRMS m/z: calcd for $C_{25}H_{26}N_9Pt$, $[M + H]^+$, 647.1955; found, 647.1931.

Synthesis of ***7a***. $HNMe_2$·HCl (106 mg, 1.30 mmol), $Ti(O^iPr)_4$ (0.40 mL, 1.24 mmol), and Et_3N (0.40 mL) were added to a solution

https://doi.org/10.1021/acs.inorgchem.3c00650
Inorg. Chem. 2023, 62, 8232−8248

of aldehyde **6** (300 mg, 0.62 mmol) in 20 mL of ethanol. The mixture was stirred at rt for 24 h. Next, $NaBH_3CN$ (59 mg, 0.93 mmol) was added, and the mixture was stirred at rt for an additional 24 h. The reaction mixture was quenched with water and extracted with DCM. The organic layers were dried over Na_2SO_4, and the solvent was evaporated under reduced pressure to yield **7a** (colorless oil) (315 mg, 99%). ^{1}H NMR (300 MHz, $CDCl_3$), δ (ppm): 8.98 (s, 1H, CH2), 8.72−8.68 (m, 1H, CH_{arom}), 8.62 (br s, 1H, CH_{arom}), 8.34 (s, 1H, CH8), 7.57−7.52 (m, 2H, CH_{arom}), 7.24−7.14 (m, 5H, CH_{arom}), 6.29 (d, J = 2.4 Hz, 1H, $CH_{anomeric}$), 5.39 (dd, J = 6.4, 2.5 Hz, 1H, CH), 5.00 (dd, J = 6.0, 2.5 Hz, 1H, CH), 4.58 (br s, 1H, CH), 4.47 (d, J = 3.9 Hz, 2H, $PhCH_2O$), 3.75 −3.56 (m, 4H, CH_2N, OCH_2CH), 2.33 (s, 6H, $N(CH_3)_2$), 1.65 (s, 3H, CH_3), 1.42 (s, 3H, CH_3). ^{13}C NMR (75 MHz, $CDCl_3$), δ (ppm): 154.9 ($C_{quaternary}$), 152.5 (C2), 151.9 ($C_{quaternary}$), 143.2 (C8), 138.6 ($C_{quaternary}$), 137.1 ($C_{quaternary}$), 135.8 ($C_{quaternary}$), 132.1 (C_{arom}), 131.8 ($C_{quaternary}$), 130.5 (C_{arom}), 129.3 (C_{arom}), 128.9 (C_{arom}), 128.5 (C_{arom}), 128.1 (C_{arom}), 127.8 (C_{arom}), 114.3 ($C_{quaternary}$), 92.1 ($CH_{anomeric}$), 86.4 (CH), 85.1 (CH), 82.2 (CH), 73.7 ($PhCH_2O$), 70.4 (CH_2N), 64.2 (OCH_2CH), 45.2 ($N(CH_3)_{2(amina)}$), 27.3 (CH_3), 25.5 (CH_3). IR (film) ν (cm^{-1}): 2928, 1747, 1577, 1221. ESI-HRMS m/z: calcd for $C_{29}H_{34}N_5O_4$, $[M + H]^+$, 516.2605; found, 516.2610.

Synthesis of ***7b****.* *p*-Anisidine (49 mg, 0.40 mmol) was added to a solution of aldehyde **6** (194 mg, 0.40 mmol) in 10 mL of DCM that contains $MgSO_4$ (10% w/w). The mixture was stirred at room temperature for 24 h. Then, $MgSO_4$ was filtered off, and the solvent was removed under reduced pressure to yield **7b** as a white solid (237 mg, 100%). ^{1}H NMR (300 MHz, $CDCl_3$), δ (ppm): 9.15 (t, J = 2.0 Hz, 1H, CH_{arom}), 9.02 (s, 1H, CH2), 8.89 (dt, J = 8.1, 1.4 Hz, 1H, CH_{arom}), 8.66 (s, 1H, CH═N), 8.38 (s, 1H, CH8), 8.18 (dt, J = 7.6, 1.4 Hz, 1H, CH_{arom}), 7.67 (t, J = 7.8 Hz, 1H, CH_{arom}), 7.30 (d, J = 8.3 Hz, 2H, CH_{arom}), 7.24−7.13 (m, 5H, CH_{arom}), 6.95 (d, J = 8.7 Hz, 2H, CH_{arom}), 6.31 (d, J = 2.3 Hz, 1H, $CH_{anomeric}$), 5.41 (dd, J = 6.1, 2.8 Hz, 1H, CH), 5.01 (dd, J = 6.1, 2.7 Hz, 1H, CH), 4.60 (br s, 1H, CH), 4.47 (d, J = 3.0 Hz, 2H, $PhCH_2O$), 3.85 (s, 3H, OCH_3), 3.74 and 3.65 (dd, J = 10.0, 3.4 Hz, 2H, OCH_2CH), 1.66 (s, 3H, CH_3), 1.43 (s, 3H, CH_3). ^{13}C NMR (75 MHz, $CDCl_3$), δ (ppm): 158.5 ($C_{quaternary}$), 158.2 (C═N), 154.1 ($C_{quaternary}$), 152.6 (C2), 152.1 ($C_{quaternary}$), 145.0 ($C_{quaternary}$), 143.3 (C8), 137.1 ($C_{quaternary}$), 137.1 ($C_{quaternary}$), 136.3 ($C_{quaternary}$), 132.5 (C_{arom}), 131.8 ($C_{quaternary}$), 130.9 (C_{arom}), 130.0 (C_{arom}), 129.3 (C_{arom}), 128.5 (C_{arom}), 128.1 (C_{arom}), 127.8 (C_{arom}), 122.5 (C_{arom}), 114.5 (C_{arom}), 114.3 ($C_{quaternary}$), 92.3 ($CH_{anomeric}$), 86.5 (CH), 85.2 (CH), 82.2 (CH), 73.7 ($PhCH_2O$), 70.4 (OCH_2CH), 55.6 (OCH_3), 27.4 (CH_3), 25.5 (CH_3). IR (film) ν (cm^{-1}): 2953, 2836, 1748, 1241, 1221. ESI-HRMS m/z: calcd for $C_{34}H_{34}N_5O_5$, $[M + H]^+$, 592.2554; found, 592.2547.

Synthesis of ***8a****.* A solution of **7a** (201 mg, 0.39 mmol) in 35 mL of dry toluene was bubbled with argon. Then, $PtCl_2(DMSO)_2$ (173 mg, 0.39 mmol) was added, and the mixture was refluxed under argon for 4 days. The solvent was removed under reduced pressure, and the residue was purified by flash SiO_2 chromatography ($CHCl_3$/ethyl acetate, 4:6) to yield **8a** (brilliant yellow solid) (134 mg, 49%). ^{1}H NMR (500 MHz, CD_2Cl_2), δ (ppm): 9.35 (s, $J(^1H-^{195}Pt)$ = 13.2 Hz, 1H, CH2), 8.38 (s, 1H, CH8), 8.20 (d, J = 7.9 Hz, 1H, CH_{arom}), 7.26−7.15 (m, 6H, CH_{arom}), 7.06 (d, J = 7.6 Hz, 1H, CH_{arom}), 6.24 (d, J = 1.8 Hz, 1H, $CH_{anomeric}$), 5.35 (dd, J = 5.8, 2.8 Hz, 1H, CH), 4.98 (dd, J = 6.1, 2.4 Hz, 1H, CH), 4.58 (br s, 1H, CH), 4.44 (d, J = 3.4 Hz, 2H, $PhCH_2O$), 4.25 (s, $J(^1H-^{195}Pt)$ = 22.0 Hz, 2H, NCH_2), 3.73 and 3.62 (dd, J = 10.3, 2.6 Hz, 2H, OCH_2CH), 3.22 (d, J = 5.6 Hz, $J(^1H-^{195}Pt)$ = 20.4 Hz, 6H, $N(CH_3)_2$), 1.62 (s, 3H, CH_3), 1.40 (s, 3H, CH_3). ^{13}C NMR (126 MHz, CD_2Cl_2), δ (ppm): 166.5 (C−Pt), 158.0 ($C_{quaternary}$), 154.8 (C2), 152.6 ($C_{quaternary}$), 146.1 (C8), 144.5 ($C_{quaternary}$), 139.0 ($C_{quaternary}$), 137.8 ($C_{quaternary}$), 130.4 ($C_{quaternary}$), 128.9 (C_{arom}), 128.5 (C_{arom}), 128.4 (C_{arom}), 128.3 (C_{arom}), 126.0 (C_{arom}), 123.8 (C_{arom}), 114.6 ($C_{quaternary}$), 92.8 ($CH_{anomeric}$), 87.2 (CH), 85.6 (CH), 82.7 (CH), 78.6 ($PhCH_2O$), 74.0 (NCH_2), 71.0 (OCH_2CH), 54.7 ($N(CH_3)_2$), 27.5 (CH_3), 25.6 (CH_3). IR (film) ν (cm^{-1}): 2926, 1602, 1575. ESI-HRMS m/z: calcd for $C_{29}H_{32}N_5O_4Pt$, $[M-Cl]^+$, 709.2099; found, 709.2090.

Synthesis of ***8b****.* As for **8a**, from **7a** (189 mg, 0.32 mmol) in 32 mL of dry toluene and $PtCl_2(DMSO)_2$ (141 mg, 0.32 mmol). The mixture was refluxed under argon for 5 days. The solvent was removed under reduced pressure, and the residue was purified by flash SiO_2 chromatography ($CHCl_3$/ethyl acetate, 2:8) to yield **8b** as a yellow solid (66 mg, 28%). ^{1}H NMR (300 MHz, $CDCl_3$), δ (ppm): 9.55 (s, $J(^1H-^{195}Pt)$ = 12.3 Hz, 1H, CH8), 9.02 (s, 1H, CH2), 8.58 (dd, J = 7.9, 1.6 Hz, $J(^1H-^{195}Pt)$ = 11.8 Hz, 1H, CH_{arom}), 8.34 (s, $J(^1H-^{195}Pt)$ = 58.0 Hz, 1H, CH═N), 7.65 (dd, J = 7.6, 1.7 Hz, 1H, CH_{arom}), 7.47 (d, J = 8.9 Hz, 2H, CH_{arom}), 7.38 (t, J = 7.8 Hz, 1H, CH_{arom}), 7.02−6.84 (m, 7H, CH_{arom}), 6.32 (d, J = 1.9 Hz, 1H, $CH_{anomeric}$), 5.40 (dd, J = 5.9, 1.8 Hz, 1H, CH), 4.90 (d, J = 6.3 Hz, 1H, CH), 4.71 (br s, 1H, CH), 4.57 and 4.32 (d, J = 11.7 Hz, 2H, $PhCH_2O$), 3.86 (s, 3H, OCH_3), 3.78−3.59 (m, 2H, OCH_2CH), 1.64 (s, 3H, CH_3), 1.44 (s, 3H, CH_3). ^{13}C NMR (75 MHz, $CDCl_3$), δ (ppm): 177.4 (C═N), 159.3 (C−Pt), 155.0 ($C_{quaternary}$), 153.7 (C2), 150.2 ($C_{quaternary}$), 149.2 ($C_{quaternary}$), 147.4 ($C_{quaternary}$), 144.7 (C8), 142.5 ($C_{quaternary}$), 136.8 ($C_{quaternary}$), 132.0 (C_{arom}), 129.7 (C_{arom}), 128.5 ($C_{quaternary}$), 128.0 (C_{arom}), 127.7 (C_{arom}), 127.6 (C_{arom}), 125.4 (C_{arom}), 123.8 (C_{arom}), 121.6 ($C_{quaternary}$), 113.9 ($C_{quaternary}$), 113.5 (C_{arom}), 94.8 ($CH_{anomeric}$), 87.7 (CH), 85.0 (CH), 82.6 (CH), 73.3 ($PhCH_2O$), 70.4 (OCH_2CH), 55.6 (OCH_3), 27.2 (CH_3), 25.5 (CH_3). IR (film) ν (cm^{-1}): 2953, 2836, 1748, 1241, 1221. ESI-HRMS m/z: calcd for $C_{34}H_{32}N_5O_5Pt$, $[M - Cl]^+$, 785.2048; found, 785.2025.

Synthesis of ***10a****.* Freshly prepared **9** (34 mg, 0.08 mmol) was added to a solution of 4 mg (0.08 mmol) of NaOH in 3 mL of MeOH, and the mixture was stirred at rt for 30 min. Then, **8a** (30 mg, 0.04 mmol) was added, and the reaction mixture was stirred at rt for 24 h. The solvent was removed under reduced pressure, and the residue was purified by flash SiO_2 chromatography ($CHCl_3$/ethyl acetate, 1:9) to yield **10a** as an orange solid (27 mg, 57%). ^{1}H NMR (500 MHz, CD_2Cl_2), δ (ppm): 9.54 (s, $J(^1H-^{195}Pt)$ = 9.8 Hz, 1H, CH2), 8.72 (s, 1H, CH2′), 8.37 (s, 1H, CH8), 8.27 (d, J = 7.2 Hz, 1H, CH_{arom}), 8.24 (s, 1H, CH8′), 7.35−7.14 (m, 12H, CH_{arom}), 6.23 (d, J = 2.4 Hz, 1H, $CH_{anomeric}$), 6.21 (d, J = 2.4 Hz, 1H, $CH_{anomeric}$), 5.37−5.33 (m, 2H, 2CH), 5.01 (dd, J = 5.7, 2.1 Hz, 1H, CH), 4.96 (dd, J = 5.7, 2.3 Hz, 1H, CH), 4.58 (br s, 1H, CH), 4.53−4.51 (br s, 1H, CH), 4.49 (d, J = 9.2 Hz, 2H, $PhCH_2O$), 4.43 (d, J = 3.4 Hz, 2H, $PhCH_2O$), 4.38 (br s, 2H, NCH_2), 3.74−3.69 (m, 2H, OCH_2CH), 3.63−3.59 (m, 2H, OCH_2CH), 3.43 (d, J = 6.0 Hz, $J(^1H-^{195}Pt)$ = 13.2 Hz, 6H, $N(CH_3)_2$), 1.63 (s, 3H, CH_3), 1.62 (s, 3H, CH_3), 1.39 (s, 3H, CH_3) and 1.38 (s, 3H, CH_3). ^{13}C NMR (126 MHz, CD_2Cl_2), δ (ppm): 176.4 (C−Pt), 138.5 (C−Pt), 157.7 (C2), 156.0 ($C_{quaternary}$), 153.1 (C2), 152.3 ($C_{quaternary}$), 150.8 ($C_{quaternary}$), 147.2 ($C_{quaternary}$), 145.9 (C8), 145.7 ($C_{quaternary}$), 142.7 (C8), 141.6 ($C_{quaternary}$), 138.2 ($C_{quaternary}$), 137.7 ($C_{quaternary}$), 135.7 ($C_{quaternary}$), 130.8 ($C_{quaternary}$), 128.9 ($2C_{arom}$), 128.5 (C_{arom}), 128.4 ($2C_{arom}$), 128.3 ($2C_{arom}$), 125.5 (C_{arom}), 124.6 (C_{arom}), 114.5 ($2C_{quaternary}$), 106.9 ($C_{quaternary}$), 93.0 and 92.0 ($CH_{anomeric}$), 87.2 and 86.7 (CH), 85.7 and 85.4 (CH), 82.7 (2CH), 80.8 (NCH_2), 74.0 ($2PhCH_2O$), 71.0 and 70.9 (CH_2), 56.7 ($N(CH_2)_3$), 27.5, 27.4, 25.7, and 25.6 (CH_3). IR (film) ν (cm^{-1}): 2074, 1574, 1479. ESI-HRMS m/z: calcd for $C_{51}H_{54}N_9O_8Pt$, $[M + H]^+$, 1115.3741; found, 1115.3737.

Synthesis of ***10b****.* As for **10a**, from a solution of 4 mg (0.09 mmol) of NaOH in 3 mL of MeOH, 35 mg (0.09 mmol) of **9**, and 35 mg (0.04 mmol) of **8b**. Purification of the crude product by SiO_2 flash chromatography ($CHCl_3$/ethyl acetate, 5:95 and 1% MeOH) yielded **10b** (orange solid) (21 mg, 41%). ^{1}H NMR (500 MHz, CD_2Cl_2), δ (ppm): 9.96 (s, $J(^1H-^{195}Pt)$ = 12.2 Hz, 1H, CH8), 9.00 (s, 1H, CH2), 8.75 (br s, 1H, CH_{arom}), 8.74 (s, 1H, CH2′), 8.61 (s, $J(^1H-^{195}Pt)$ = 54.7 Hz, 1H, CH═N), 8.26 (s, 1H, CH8′), 7.79−7.75 (m, 3H, CH_{arom}), 7.43 (t, J = 7.3 Hz, 1H, CH_{arom}), 7.30−7.22 (m, 5H, CH_{arom}), 6.99−6.87 (m, 7H, CH_{arom}), 6.35 (d, J = 2.0 Hz, 1H, $CH_{anomeric}$), 6.22 (d, J = 2.0 Hz, 1H, $CH_{anomeric}$), 5.52 (d, J = 5.5 Hz, 1H, CH), 5.37 (dd, J = 7.1, 2.7 Hz, 1H, CH), 5.01 (dd, J = 6.0, 2.0 Hz, 2H, 2CH), 4.60 (br s, 1H, CH), 4.56−4.52 (m, 1H, CH), 4.51−4.29 (m, 4H, $PhCH_2O$), 3.80 (s, 3H, OCH_3), 3.79 (dd, J = 10.6, 3.0 Hz, 1H, OCH_2CH), 3.71 (dd, J = 10.6, 3.0 Hz, 1H, OCH_2CH), 3.63 (dd, J = 10.6, 3.9 Hz, 1H, OCH_2CH), 3.47 (dd, J = 10.6, 3.9 Hz, 1H,

https://doi.org/10.1021/acs.inorgchem.3c00650
Inorg. Chem. 2023, 62, 8232−8248

OCH_2CH), 1.63 (s, 6H, CH_3), 1.44 (s, 3H, CH_3) and 1.40 (s, 3H, CH_3). ^{13}C NMR (126 MHz, CD_2Cl_2), δ (ppm): 179.7 (C=N), 170.6 (C−Pt), 159.8 (C−Pt), 157.2 ($C_{quaternary}$), 154.0 (C2), 153.2 (C2), 150.9 ($C_{quaternary}$), 150.5 ($C_{quaternary}$), 149.4 ($C_{quaternary}$), 148.5 (C8), 145.5 ($C_{quaternary}$), 144.9 ($C_{quaternary}$), 142.7 (C8), 138.1 ($C_{quaternary}$), 137.7 ($C_{quaternary}$), 135.9 ($C_{quaternary}$), 132.0 (C_{arom}), 131.0 ($C_{quaternary}$), 129.1 (C_{arom}), 129.0 (C_{arom}), 128.5 (C_{arom}), 128.4 (C_{arom}), 128.3 (C_{arom}), 128.1 ($C_{quaternary}$), 128.1 (C_{arom}), 127.8 (C_{arom}), 126.0 (C_{arom}), 125.0 (C_{arom}), 122.3 ($C_{quaternary}$), 114.6 ($C_{quaternary}$), 114.1 ($C_{quaternary}$), 113.9 (C_{arom}), 105.5 ($C_{quaternary}$), 95.0 and 92.0 ($CH_{anomeric}$), 88.5 and 86.6 (CH), 86.0 and 85.3 (CH), 83.3 and 82.7 (CH), 74.0 and 73.4 ($PhCH_2O$), 70.9 and 70.7 (OCH_2CH), 56.0 (OCH_3), 27.5 and 27.4 (CH_3), 25.7 ($2CH_3$). IR (film) ν (cm^{-1}): 2927, 2083, 1604, 1572. ESI-HRMS *m/z*: calcd for $C_{56}H_{54}N_9O_9Pt$, $[M + H]^+$, 1192.3705; found, 1192.3701.

■ ASSOCIATED CONTENT

Supporting Information

The Supporting Information is available free of charge at https://pubs.acs.org/doi/10.1021/acs.inorgchem.3c00650.

Synthesis and characterization of compounds **6** and **9**; computed frontier orbitals and their energies; XRD data, absorption, and emission spectra and NMR spectra (PDF)

Cartesian coordinates (TXT)

Accession Codes

CCDC deposition numbers: 2242639 (**3a**·0.5($CHCl_3$)), 2242640 (**3b**), 2242641 (**3c**·0.5(CH_2Cl_2)), 2242642 (**3d**), 2242643 (**4b**), 2242644 (**4d**), and 2242645 (**5a**), contain the supporting crystallographic data for this paper. These data can be obtained free of charge *via* www.ccdc.cam.ac.uk/data_request/cif, by emailing data_request@ccdc.cam.ac.uk, or by contacting The Cambridge Crystallographic Data Center, 12 Union Road, Cambridge CB2 1EZ, U.K.; fax: +44 1223 336033.

■ AUTHOR INFORMATION

Corresponding Authors

Mar Gómez Gallego − *Departamento de Química Orgánica, Facultad de Ciencias Químicas, Universidad Complutense, 28040 Madrid, Spain; Center for Innovation in Advanced Chemistry (ORFEO-CINQA)*, https://orfeocinqa.es/; orcid.org/0000-0002-8961-7685; Email: margg@quim.ucm.es

Miguel A. Sierra − *Departamento de Química Orgánica, Facultad de Ciencias Químicas, Universidad Complutense, 28040 Madrid, Spain; Center for Innovation in Advanced Chemistry (ORFEO-CINQA)*, https://orfeocinqa.es/; orcid.org/0000-0002-3360-7795; Email: sierraor@quim.ucm.es

Authors

Carmen Lorenzo-Aparicio − *Departamento de Química Orgánica, Facultad de Ciencias Químicas, Universidad Complutense, 28040 Madrid, Spain; Center for Innovation in Advanced Chemistry (ORFEO-CINQA)*, https://orfeocinqa.es/; orcid.org/0000-0001-8081-9726

Sonia Moreno-Blázquez − *Departamento de Química Inorgánica, Instituto de Síntesis Química y Catálisis Homogénea (ISQCH), Universidad de Zaragoza-CSIC, 50009 Zaragoza, Spain; Center for Innovation in Advanced Chemistry (ORFEO-CINQA)*, https://orfeocinqa.es/

Montserrat Oliván − *Departamento de Química Inorgánica, Instituto de Síntesis Química y Catálisis Homogénea (ISQCH), Universidad de Zaragoza-CSIC, 50009 Zaragoza, Spain; Center for Innovation in Advanced Chemistry (ORFEO-CINQA)*, https://orfeocinqa.es/; orcid.org/0000-0003-0381-0917

Miguel A. Esteruelas − *Departamento de Química Inorgánica, Instituto de Síntesis Química y Catálisis Homogénea (ISQCH), Universidad de Zaragoza-CSIC, 50009 Zaragoza, Spain; Center for Innovation in Advanced Chemistry (ORFEO-CINQA)*, https://orfeocinqa.es/; orcid.org/0000-0002-4829-7590

Pablo García-Álvarez − *Departamento de Química Orgánica e Inorgánica, Facultad de Química, Universidad de Oviedo, 33071 Oviedo, Spain; Center for Innovation in Advanced Chemistry (ORFEO-CINQA)*, https://orfeocinqa.es/

Javier A. Cabeza − *Departamento de Química Orgánica e Inorgánica, Facultad de Química, Universidad de Oviedo, 33071 Oviedo, Spain; Center for Innovation in Advanced Chemistry (ORFEO-CINQA)*, https://orfeocinqa.es/; orcid.org/0000-0001-8563-9193

Complete contact information is available at: https://pubs.acs.org/10.1021/acs.inorgchem.3c00650

Notes

The authors declare no competing financial interest.

†Dedicated to Prof. Joaquín Tamariz from Instituto Politécnico Nacional (México) on the occasion of his retirement.

■ ACKNOWLEDGMENTS

Support for this work under grants PID2019-108429RB-I00 to M.A.S., PID2020-115286GB-I00 to M.A.E., PID2019-104652GB-I00 to J.A.C., RED2018-102387-T (ORFEO-CINQA network), from the MCINN (Spain); and E06-23R and LMP23-21 to M.A.E. from the Gobierno de Aragón is gratefully acknowledged. Technical support provided by Servicios Científico-Técnicos de la Universidad de Oviedo is also acknowledged.

■ REFERENCES

(1) Selected revisions: (a) Lippert, B.; Sanz Miguel, J. P. S. Beyond sole models for the first steps of Pt-DNA interactions: Fundamental properties of mono(nucleobase) adducts of Pt(II) coordination compounds. *Coord. Chem. Rev.* **2022**, *465*, 214566. (b) Collado, A.; Gómez-Gallego, M.; Sierra, M. A. Nucleobases having M−C Bonds: An emerging bio-organometallic field. *Eur. J. Org. Chem.* **2018**, *2018*, 1617−1623. (c) Naskar, S.; Guha, R.; Müller, J. Metal-Modified Nucleic Acids: Metal-Mediated Base Pairs, Triples, and Tetrads. *Angew. Chem., Int. Ed.* **2020**, *59*, 1397−1406. (d) Müller, J. Nucleic acid duplexes with metal-mediated base pairs and their structures. *Coord. Chem. Rev.* **2019**, *393*, 37−47. (e) Jain, A. Multifunctional, heterometallic ruthenium-platinum complexes with medicinal applications. *Coord. Chem. Rev.* **2019**, *401*, No. 213067. (f) Soldevila-Barreda, J. J.; Metzler-Nolte, N. Intracellular Catalysis with Selected Metal Complexes and Metallic Nanoparticles: Advances toward the Development of Catalytic Metallodrugs. *Chem. Rev.* **2019**, *119*, 829−869. (g) Zhang, P.; Huang, H. Future potential of osmium complexes as anticancer drug candidates, photosensitizers and organelle-targeted probes. *Dalton Trans.* **2018**, *47*, 14841−14854. (h) Erxleben, A. Interactions of copper complexes with nucleic acids. *Coord. Chem. Rev.* **2018**, *360*, 92−121. (i) Bergamo, A.; Dyson, P. J.; Sava, G. The mechanism of tumour cell death by metal-based anticancer drugs is not only a matter of DNA interactions. *Coord. Chem. Rev.* **2018**, *360*, 17−33. (j) Brabec, V.; Kasparkova, J. Ruthenium coordination compounds of biological and biomedical significance. DNA binding agents. *Coord. Chem. Rev.* **2018**, *376*, 75−94. (k) Kapdi, A. R.; Fairlamb, I. J. S. Anti-cancer palladium complexes: a focus on

PdX2L2, palladacycles and related complexes. *Chem. Soc. Rev.* **2014**, *43*, 4751−4777. (l) Ma, D.-L.; Chan, D. S.-H.; Leung, C.-H. Group 9 Organometallic Compounds for Therapeutic and Bioanalytical Applications. *Acc. Chem. Res.* **2014**, *47*, 3614−3631. (m) Liu, H. K.; Sadler, P. J. Metal Complexes as DNA Intercalators. *Acc. Chem. Res.* **2011**, *44*, 349−359. (n) Clever, G. H.; Shionoya, M. Metal-base pairing in DNA. *Coord. Chem. Rev.* **2010**, *254*, 2391−2402.

(2) (a) Johnstone, T. C.; Suntharalingam, K.; Lippard, S. J. The Next Generation of Platinum Drugs: Targeted Pt(II) Agents, Nanoparticle Delivery, and Pt(IV) Prodrugs. *Chem. Rev.* **2016**, *116*, 3436−3486. (b) Dasari, S.; Tchounwou, P. B. Cisplatin in cancer therapy: Molecular mechanisms of action. *Eur. J. Pharmacol.* **2014**, *740*, 364−378.

(3) (a) Dilruba, S.; Kalayda, G. V. Platinum-based drugs: past, present and future. *Cancer Chemother. Pharmacol.* **2016**, *77*, 1103−1124. (b) Wilson, J. J.; Lippard, S. J. Synthetic Methods for the Preparation of Platinum Anticancer Complexes. *Chem. Rev.* **2014**, *114*, 4470−4495.

(4) Siddik, Z. H. Cisplatin: mode of cytotoxic action and molecular basis of resistance. *Oncogene* **2003**, *22*, 7265−7279.

(5) Jamieson, E. R.; Lippard, S. J. Structure, recognition, and processing of cisplatin-DNA adducts. *Chem. Rev.* **1999**, *99*, 2467−2498.

(6) Brabec, V.; Hrabina, O.; Kasparkova, J. Cytotoxic platinum coordination compounds. DNA binding agents. *Coord. Chem. Rev.* **2017**, *351*, 2−31.

(7) Ma, D.-L.; Che, C.-M. A Bifunctional Platinum(II) Complex Capable of Intercalation and Hydrogen-Bonding Interactions with DNA: Binding Studies and Cytotoxicity. *Chem.—Eur. J.* **2003**, *9*, 6133−6144.

(8) Georgiades, S. N.; Karim, N. H. K.; Suntharalingam, K.; Vilar, R. Interaction of Metal Complexes with G-Quadruplex DNA. *Angew. Chem., Int. Ed.* **2010**, *49*, 4020−4034.

(9) Some recent examples: (a) Savva, L.; Fossépré, M.; Keramidas, O.; Themistokleous, A.; Rizeq, N.; Panagiotou, N.; Leclercq, M.; Nicolaidou, E.; Surin, M.; Hayes, S. C.; Georgiades, S. N. Gaining Insights on the Interactions of a Class of Decorated (2-([2,2′-Bipyridin]-6-yl)phenyl)platinum Compounds with c-Myc Oncogene Promoter G-Quadruplex and Other DNA Structures. *Chem.—Eur. J.* **2022**, *28*, No. e202201497. (b) Zhu, B.-C.; He, J.; Liu, W.; Xia, X.-Y.; Liu, L.-Y.; Liang, B.-B.; Yao, H.-G.; Liu, B.; Ji, L.-N.; Mao, Z.-W. Selectivity and Targeting of G-Quadruplex Binders Activated by Adaptive Binding and Controlled by Chemical Kinetics. *Angew. Chem. Int Ed.,* **2021**, *60*, 15340−15343. (c) Cao, Q.; Li, Y.; Freisinger, E.; Qin, P. Z.; Sigel, R. K. O.; Mao, Z.-W. G-quadruplex DNA targeted metal complexes acting as potential anticancer drugs. *Inorg. Chem. Front.* **2017**, *4*, 10−32. (d) Ang, D. L.; Harper, B. W. J.; Cubo, L.; Mendoza, O.; Vilar, R.; Aldrich-Wright, J. Quadruplex DNA-Stabilising Dinuclear Platinum(II) Terpyridine Complexes with Flexible Linkers. *Chem.—Eur. J.* **2016**, *22*, 2317−2325.

(10) (a) Clauson, C.; Scharer, O. D.; Niedernhofer, L. Advances in understanding the complex mechanisms of DNA interstrand cross-link repair. *Cold Spring Harbor Perspect. Biol.* **2013**, *5*, No. a012732. (b) Brulikova, A. L.; Hlavac, J.; Hradil, P. DNA interstrand cross-linking agents and their chemotherapeutic potential. *Curr. Med. Chem.* **2012**, *19*, 364−385. (c) Osawa, T.; Davies, D.; Hartley, J. A. Mechanism of Cell Death Resulting from DNA Interstrand Cross-Linking in Mammalian Cells. *Cell Death Dis.* **2011**, *2*, No. e187. (d) Deans, A. J.; West, S. C. DNA interstrand crosslink repair and cancer. *Nat. Rev. Cancer* **2011**, *11*, 467−480. (e) Noll, D. M.; Mason, T. M.; Miller, P. S. Formation and repair of interstrand cross-links in DNA. *Chem. Rev.* **2006**, *106*, 277−301.

(11) Haque, A.; Xu, L.; Al-Balushi, R. A.; Al-Suti, M. K.; Ilmi, R.; Guo, Z.; Khan, M. S.; Wong, W.-Y.; Raithby, P. R. Cyclometallated tridentate platinum(II) arylacetylide complexes: old wine in new bottles. *Chem. Soc. Rev.* **2019**, *48*, 5547−5563.

(12) Yam, V. W.-W.; Au, K.-M. V.; Leung, S. Y.-L. Light-Emitting Self-Assembled Materials Based on d^8 and d^{10} Transition Metal Complexes. *Chem. Rev.* **2015**, *115*, 7589−7772.

(13) Li, K.; Tong, G. S. M.; Wan, Q.; Cheng, G.; Tong, W.-Y.; Ang, W.-H.; Kwong, W.-L.; Che, C.-M. Highly phosphorescent platinum(II) emitters: photophysics, materials and biological applications. *Chem. Sci.* **2016**, *7*, 1653−1673.

(14) Williams, J. A. G. The coordination chemistry of dipyridylbenzene: N-deficient terpyridine or panacea for brightly luminescent metal complexes? *Chem. Soc. Rev.* **2009**, *38*, 1783−1801.

(15) Guha, R.; Defayay, D.; Hepp, A.; Müller, J. Targeting Guanine Quadruplexes with Luminescent Platinum(II) Complexes Bearing a Pendant Nucleobase. *ChemPlusChem* **2021**, *86*, 662−673.

(16) (a) Chan, K.; Chung, C. Y.-S.; Yam, V. W.-W. Parallel folding topology-selective label-free detection and monitoring of conformational and topological changes of different G-quadruplex DNAs by emission spectral changes via FRET of mPPE-Ala−Pt(II) complex ensemble. *Chem. Sci.* **2016**, *7*, 2842−2855. (b) Wang, P.; Leung, C.-H.; Ma, D.-L.; Yan, S.-C.; Che, C.-M. Structure-Based Design of Platinum(II) Complexes as c-*myc* Oncogene Down-Regulators and Luminescent Probes for G-Quadruplex DNA. *Chem.—Eur. J.* **2010**, *16*, 6900−6911.

(17) Botchway, S. W.; Charnley, M.; Haycock, J. W.; Parker, A. W.; Rochester, D. L.; Weinstein, J. A.; Williams, J. A. G. Time-resolved and two-photon emission imaging microscopy of live cells with inert platinum complexes. *Proc. Natl. Acad. Sci. U.S.A.* **2008**, *105*, 16071−16076.

(18) (a) Martín-Ortíz, M.; Gómez-Gallego, M.; Ramírez de Arellano, C.; Sierra, M. A. The Selective Synthesis of Metallanucleosides and Metallanucleotides: A New Tool for the Functionalization of Nucleic Acids. *Chem.—Eur. J.* **2012**, *18*, 12603−12608. (b) Valencia, M.; Martín-Ortiz, M.; Gómez-Gallego, M.; Ramírez de Arellano, C.; Sierra, M. A. On the Use of Metal Purine Derivatives (M = Ir, Rh) for the Selective Labeling of Nucleosides and Nucleotides. *Chem.—Eur. J.* **2014**, *20*, 3831−3838.

(19) Giner, E. A.; Gómez-Gallego, M.; Merinero, A. D.; Casarrubios, L.; Ramírez de Arellano, C.; Sierra, M. A. Sequential Reactions of Alkynes on an Iridium(III) Single Site. *Chem.—Eur. J.* **2017**, *23*, 8941−8948.

(20) Valencia, M.; Merinero, A. D.; Lorenzo-Aparicio, C.; Gómez-Gallego, M.; Sierra, M. A.; Eguillor, B.; Esteruelas, M. A.; Oliván, M.; Oñate, E. Osmium-Promoted σ-Bond Activation Reactions on Nucleosides. *Organometallics* **2020**, *39*, 312−323.

(21) Lorenzo-Aparicio, C.; Gómez-Gallego, M.; Ramírez de Arellano, C.; Sierra, M. A. Phosphorescent Ir(III) complexes derived from purine nucleobases. *Dalton Trans.* **2022**, *51*, 5138−5150.

(22) Sinha, I.; Hepp, A.; Schirmer, B.; Kösters, J.; Neugebauer, J.; Müller, J. Regioselectivity of the C-Metalation of 6-Furylpurine: Importance of Directing Effects. *Inorg. Chem.* **2015**, *54*, 4183−4185.

(23) Cárdenas, D. J.; Echavarren, A. M.; Ramírez de Arellano, M. C. Divergent Behavior of Palladium(II) and Platinum(II) in the Metalation of 1,3-Di(2-pyridyl)benzene. *Organometallics* **1999**, *18*, 3337−3341.

(24) A search in the Cambridge Structure Database (CSD version 2022.2.0; updated June 2022) for pincer complexes of the type [Pt(κ^3*N*,*C*,*N*-ligand)X] (X = Cl, alkynyl) gave average Pt—N, Pt—C(arene), Pt—Cl and Pt—C(alkynyl) bond distances of *ca.* 2.04, 1.93, 2.41 and 2.06 Å, respectively.

(25) It should be noted that, for **3a** and **3c**, the crystals also contain $CHCl_3$ and CH_2Cl_2, respectively, as co-crystallization solvents, which could also affect the molecular packing.

(26) Alvarez, S. A. Cartography of the van der Waals territories. *Dalton Trans.* **2013**, *42*, 8617−8636.

(27) A search in the Cambridge Structure Database (CSD version 2022.2.0; updated June 2022) for PhC≡CX (X not a transition metal) compounds gave an average C≡C bond distance of 1.20(2) Å.

(28) (a) Williams, J. A. G.; Develay, S.; Rochester, D. L.; Murphy, L. Optimising the luminescence of platinum(II) complexes and their application in organic light emitting devices (OLEDs). *Coord. Chem. Rev.* **2008**, *252*, 2596−2611. (b) Huo, S.; Carroll, J.; Vezzu, D. A. K. Design, Synthesis, and Applications of Highly Phosphorescent Cyclometalated Platinum Complexes. *Asian J. Org. Chem.* **2015**, *4*,

https://doi.org/10.1021/acs.inorgchem.3c00650
Inorg. Chem. 2023, 62, 8232−8248

1210−1245. (c) Yam, V. W.-W.; Law, A. S.-Y. Luminescent d^8 metal complexes of platinum(II) and gold(III): From photophysics to photofunctional materials and probes. *Coord. Chem. Rev.* **2020**, *414*, No. 213298.

(29) (a) Pettijohn, C. N.; Jochnowitz, E. B.; Chuong, B.; Nagle, J. K.; Vogler, A. Luminescent excimers and exciplexes of Pt^{II} compounds. *Coord. Chem. Rev.* **1998**, *171*, 85−92. (b) Crites Tears, D. K.; McMillin, D. R. Exciplex quenching of photoexcited platinum(II) terpyridines: influence of the orbital parentage. *Coord. Chem. Rev.* **2001**, *211*, 195−205.

(30) (a) Eguillor, B.; Esteruelas, M. A.; Lezáun, V.; Oliván, M.; Oñate, E. Elongated Dihydrogen versus Compressed Dihydride in Osmium Complexes. *Chem.—Eur. J.* **2017**, *23*, 1526−1530. (b) Castro-Rodrigo, R.; Esteruelas, M. A.; Gómez-Bautista, D.; Lezáun, V.; López, A. M.; Oñate, E. Influence of the Bite Angle of Dianionic C,N,C-Pincer Ligands on the Chemical and Photophysical Properties of Iridium(III) and Osmium(IV) Hydride Complexes. *Organometallics* **2019**, *38*, 3707−3718.

(31) (a) Lai, S.-W.; Chan, M. C.-W.; Cheung, T.-C.; Peng, S.-M.; Che, C.-M. Probing d^8-d^8 Interactions in Luminescent Mono- and Binuclear Cyclometalated Platinum(II) Complexes of 6-Phenyl-2,2′-bipyridines. *Inorg. Chem.* **1999**, *38*, 4046−4055. (b) Mróz, W.; Botta, C.; Giovanella, U.; Rossi, E.; Colombo, A.; Dragonetti, C.; Roberto, D.; Ugo, R.; Valore, A.; Williams, J. A. G. Cyclometallated platinum(II) complexes of 1,3-di(2-pyridyl)benzenes for solution-processable WOLEDs exploiting monomer and excimer phosphorescence. *J. Mater. Chem.* **2011**, *21*, 8653−8661. (c) Rossi, E.; Colombo, A.; Dragonetti, C.; Roberto, D.; Ugo, R.; Valore, A.; Falciola, L.; Brulatti, P.; Cocchi, M.; Williams, J. A. G. Novel N∧C∧N-cyclometallated platinum complexes with acetylide co-ligands as efficient phosphors for OLEDs. *J. Mater. Chem.* **2012**, *22*, 10650−10655. (d) Li, K.; Zou, T.; Chen, Y.; Guan, X.; Che, C.-M. Pincer-Type Platinum(II) Complexes Containing N-Heterocyclic Carbene (NHC) Ligand: Structures, Photophysical and Anion Binding Properties, and Anticancer Activities. *Chem.—Eur. J.* **2015**, *21*, 7441−7453. (e) Bachmann, M.; Suter, D.; Blacque, O.; Venkatesan, K. Tunable and Efficient White Light Phosphorescent Emission Based on Single Component N-Heterocyclic Carbene Platinum(II) Complexes. *Inorg. Chem.* **2016**, *55*, 4733−4745. (f) Martínez-Junquera, M.; Lara, R.; Lalinde, E.; Moreno, M. T. Isomerism, aggregation-induced emission and mechanochromism of isocyanide cycloplatinated(II) complexes. *J. Mater. Chem. C* **2020**, *8*, 7221−7233. (g) Pander, P.; Sil, A.; Salthouse, R. J.; Harris, C. W.; Walden, M. T.; Yufit, D. S.; Williams, J. A. G.; Dias, F. B. Excimer or aggregate? Near infrared electro- and photoluminescence from multimolecular excited states of N∧C∧N-coordinated platinum(II) complexes. *J. Mater. Chem. C* **2022**, *10*, 15084−15095. (h) Lázaro, A.; Bosque, R.; Ward, J. S.; Rissanen, K.; Crespo, M.; Rodríguez, L. Toward Near Infrared Emission in Pt(II)-Cyclometallated Compounds: From Excimers' Formation to Aggregation-Induced Emission. *Inorg. Chem.* **2023**, *62*, 2000−2012.

(32) (a) Wan, K.-T.; Che, C.-M.; Cho, K.-C. Inorganic Excimer. Spectroscopy, Photoredox Properties and Excimeric Emission of Dicyano(4,4′-di-tert-butyl-2,2′-bipyridine)platinum(II). *J. Chem. Soc., Dalton Trans.* **1991**, 1077−1080. (b) Farley, S. J.; Rochester, D. L.; Thompson, A. L.; Howard, J. A. K.; Williams, J. A. G. Controlling Emission Energy, Self-Quenching, and Excimer Formation in Highly Luminescent N∧C∧N-Coordinated Platinum(II) Complexes. *Inorg. Chem.* **2005**, *44*, 9690−9703. (c) Develay, S.; Blackburn, O.; Thompson, A. L.; Williams, J. A. G. Cyclometalated Platinum(II) Complexes of Pyrazole-Based, N∧C∧N-Coordinating, Terdentate Ligands: the Contrasting Influence of Pyrazolyl and Pyridyl Rings on Luminescence. *Inorg. Chem.* **2008**, *47*, 11129−11142. (d) Tanaka, S.; Sato, K.; Ichida, K.; Abe, T.; Tsubomura, T.; Suzuki, T.; Shinozaki, K. Circularly Polarized Luminescence of Chiral Pt(pppb)Cl (pppbH =1-pyridyl-3-(4,5-pinenopyridyl)benzene) Aggregate in the Excited State. *Chem.—Asian J.* **2016**, *11*, 265−273.

(33) (a) Connick, W. B.; Geiger, D.; Eisenberg, R. Excited-State Self-Quenching Reactions of Square Planar Platinum(II) Diimine Complexes in Room-Temperature Fluid Solution. *Inorg. Chem.* **1999**, *38*, 3264−3265. (b) Williams, J. A. G.; Beeby, A.; Davies, E. S.; Weinstein, J. A.; Wilson, C. An Alternative Route to Highly Luminescent Platinum(II) Complexes: Cyclometalation with N∧C∧N-Coordinating Dipyridylbenzene Ligands. *Inorg. Chem.* **2003**, *42*, 8609−8611.

(34) (a) Connick, W. B.; Gray, H. B. Photooxidation of Platinum(II) Diimine Dithiolates. *J. Am. Chem. Soc.* **1997**, *119*, 11620−11627. (b) Vezzu, D. A. K.; Deaton, J. C.; Jones, J. S.; Bartolotti, L.; Harris, C. F.; Marchetti, A. P.; Kondakova, M.; Pike, R. D.; Huo, S. Highly Luminescent Tetradentate Bis-Cyclometalated Platinum Complexes: Design, Synthesis, Structure, Photophysics, and Electroluminescence Application. *Inorg. Chem.* **2010**, *49*, 5107−5119. (c) Harris, C. F.; Vezzu, D. A. K.; Bartolotti, L.; Boyle, P. D.; Huo, S. Synthesis, Structure, Photophysics, and a DFT Study of Phosphorescent C*N∧N- and C∧N∧N-Coordinated Platinum Complexes. *Inorg. Chem.* **2013**, *52*, 11711−11722.

(35) Hruzd, M.; le Poul, N.; Cordier, M.; Kahlal, S.; Saillard, J.-Y.; Achelle, S.; Gauthier, S.; Robin-le Guen, F. Luminescent cyclometalated alkynylplatinum(II) complexes with 1,3-di(pyrimidin-2-yl)benzene ligands: synthesis, electrochemistry, photophysics and computational studies. *Dalton Trans.* **2022**, *51*, 5546−5560.

(36) Zhou, D.; Xie, D.; He, F.; Song, B.; Hu, D. Antiviral properties and interaction of novel chalcone derivatives containing a purine and benzenesulfonamide moiety. *Bioorg. Med. Chem. Lett.* **2018**, *28*, 2091−2097.

(37) Li, Z.; Li, H.; Gifford, B. J.; Peiris, W. D. N.; Kilina, S.; Sun, W. Synthesis, photophysics, and reverse saturable absorption of 7-(benzothiazol-2-yl)-9,9-di(2-ethylhexyl)-9*H*-fluoren-2-yl tethered $[Ir(bpy)(ppy)_2]PF_6$ and $Ir(ppy)_3$ complexes (bpy = 2,2′-bipyridine, ppy = 2-phenylpyridine). *RSC Adv.* **2016**, *6*, 41214−41228.

(38) Nauš, P.; Votruba, I.; Hocek, M. Covalent Analogues of DNA Base-Pairs and Triplets VII. Synthesis and Cytostatic Activity of Bis(purin-6-yl)acetylene and -diacetylene Nucleosides. *Collect. Czech. Chem. Commun.* **2004**, *69*, 1955−1970.

(39) (a) Price, J. H.; Birk, J. P.; Wayland, B. B. Thermal and photochemical cis-trans isomerization of PtL2Cl2 (L = dialkyl sulfoxide) complexes. Kinetics and mechanisms for thermal isomerization. *Inorg. Chem.* **1978**, *17*, 2245−2250. (b) Kitching, W.; Moore, C. J.; Doddrell, D. Spectroscopic studies of alkyl sulfoxide complexes of platinum(II) and palladium(II). *Inorg. Chem.* **1970**, *9*, 541−549.

(40) Frisch, M. J.; Trucks, G. W.; Schlegel, H. B.; Scuseria, G. E.; Robb, M. A.; Cheeseman, J. R.; Scalmani, G.; Barone, V.; Mennucci, B.; Petersson, G. A.; Nakatsuji, H.; Caricato, M.; Li, X.; Hratchian, H. P.; Izmaylov, A. F.; Bloino, J.; Zheng, G.; Sonnenberg, J. L.; Hada, M.; Ehara, M.; Toyota, K.; Fukuda, R.; Hasegawa, J.; Ishida, M.; Nakajima, T.; Honda, Y.; Kitao, O.; Nakai, H.; Vreven, T.; Montgomery, J. A., Jr.; Peralta, J. E.; Ogliaro, F.; Bearpark, M.; Heyd, J. J.; Brothers, E.; Kudin, K. N.; Staroverov, V. N.; Kobayashi, R.; Normand, J.; Raghavachari, K.; Rendell, A.; Burant, J. C.; Iyengar, S. S.; Tomasi, J.; Cossi, M.; Rega, N.; Millam, J. M.; Klene, M.; Knox, J. E.; Cross, J. B.; Bakken, V.; Adamo, C.; Jaramillo, J.; Gomperts, R.; Stratmann, R. E.; Yazyev, O.; Austin, A. J.; Cammi, R.; Pomelli, C.; Ochterski, J. W.; Martin, R. L.; Morokuma, K.; Zakrzewski, V. G.; Voth, G. A.; Salvador, P.; Dannenberg, J. J.; Dapprich, S.; Daniels, A. D.; Farkas, Ö.; Foresman, J. B.; Ortiz, J. V.; Cioslowski, J.; Fox, D. J. *Gaussian 09*, revision D.01; Gaussian, Inc.: Wallingford, CT, 2009.

(41) Grimme, S.; Antony, J.; Ehrlich, S.; Krieg, H. A. Consistent and accurate ab initio parametrization of density functional dispersion correction (DFT-D) for the 94 elements H-Pu. *J. Chem. Phys.* **2010**, *132*, No. 154104.

(42) Weigend, F.; Ahlrichs, R. Balanced basis sets of split valence, triple zeta valence and quadruple zeta valence quality for H to Rn: Design and assessment of accuracy. *Phys. Chem. Chem. Phys.* **2005**, *7*, 3297−3305.

(43) Marenich, A. V.; Cramer, C. J.; Truhlar, D. G. Universal Solvation Model Based on Solute Electron Density and on a Continuum Model of the Solvent Defined by the Bulk Dielectric

https://doi.org/10.1021/acs.inorgchem.3c00650
Inorg. Chem. 2023, 62, 8232−8248

Constant and Atomic Surface Tensions. *J. Phys. Chem. B* **2009**, *113*, 6378−6396.
(44) *CrysAlisPro RED*, version 1.171.38.46; Oxford Diffraction Ltd.: Oxford, U.K., 2015.
(45) SIR-97: Altomare, A.; Burla, M. C.; Camalli, M.; Cascarano, G. L.; Giacovazzo, C.; Guagliardi, A.; Moliterni, A. G. C.; Polidori, G.; Spagna, R. SIR97: A new tool for crystal structure determination and refinement. *J. Appl. Crystallogr.* **1999**, *32*, 115−119.
(46) SHELXL-2014: Sheldrick, G. M. A Short History of SHELX. *Acta Crystallogr., Sect. A: Found. Crystallogr.* **2008**, *64*, 112−122.
(47) WINGX, version 2021.3: Farrugia, L. J. WinGX and ORTEP for Windows: An Update. *J. Appl. Crystallogr.* **2012**, *45*, 849−854.
(48) *MERCURY*, version 2022.2.0 (build 353591); Cambridge Crystallographic Data Centre: Cambridge, U.K., 2022.

https://doi.org/10.1021/acs.inorgchem.3c00650
Inorg. Chem. 2023, 62, 8232−8248